ACS Partner Journal
ENVIRONMENT & HEALTH

pubs.acs.org/EnvHealth
Review

Advances in Electrostatic Plasma Methods for Purification of Airborne Pathogenic Microbial Aerosols: Mechanism, Modeling and Application

Published as part of Environment & Health virtual special issue "Grand Environmental Challenge: Indoor Air Pollution, Health Effects, and Mitigation".

Shanlong Tao, Yong Zhu,* Mingxia Chen, and Wenfeng Shangguan*

Cite This: *Environ. Health* 2024, 2, 596−617

ABSTRACT: The transmission of pathogenic airborne microorganisms significantly impacts public health and societal functioning. Ensuring healthy indoor air quality in public spaces is critical. Among various air purification technologies, electrostatic precipitation and atmospheric pressure nonthermal plasma are notable for their broad-spectrum effectiveness, high efficiency, cost-effectiveness, and safety. This review investigates the primary mechanisms by which these electrostatic methods collect and disinfect pathogenic aerosols. It also delves into recent advancements in enhancing their physical and chemical mechanisms for improve efficiency. Simultaneously, a thorough summary of mathematical models related to the migration and deactivation of pathogenic aerosols in electrostatic purifiers is provided. It will help us to understand the behavior of aerosols in purification systems. Additionally, the review discusses the current research on creating a comprehensive health protection system and addresses the challenges of balancing byproduct control with efficiency. The aim is to establish a foundation for future research and development in electrostatic aerosol purification and develop integrated air purification technologies that are both efficient and safe.

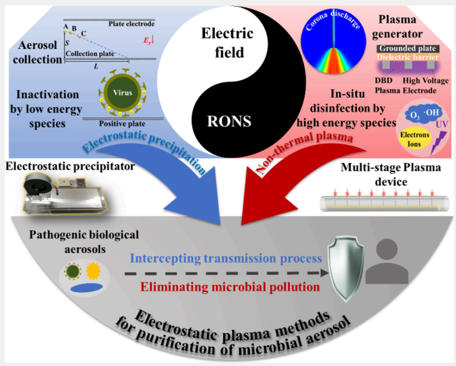

KEYWORDS: *electrostatic, microbial aerosols, inactivation, collection, air purification*

1. INTRODUCTION

The level of human health is closely related to the cleanliness of the air in the living environment.[1] According to statistics from the World Health Organization,[2] 3 million deaths worldwide in 2016 can be attributed to lower respiratory tract infections, ranking fourth among all causes of death. After entering the 21st century, large-scale respiratory infectious diseases broke out worldwide, such as the SARS virus in 2003, the H1N1 virus in 2009, and the new coronavirus in 2019, which has been causing significant damage to the health of worldwide individuals and disrupting the regular operation of the whole society.[3] There are mainly two main modes of transmission of infectious diseases in the respiratory system, aerosol transmission (particle diameter <5 μm) and droplet transmission (particle diameter >5 μm).[4,5] Generally speaking, aerosols containing pathogenic microorganisms can suspend longer and spread further than droplet transmission, which requires a quicker and more efficient method to remove and deactivate them.

As for primary purification methods for microorganisms, two main categories are listed in Figure 1. The physical techniques primarily consist of adsorption, heat, electric field, etc. These methods usually involve the collection and preliminary inactivation by physical effects. Simultaneously, the chemical methods mainly refer to the chemical reaction between microorganisms and the active species induced by photocatalysis, UV light, and nonthermal plasma. For the Heating, Ventilation, and Air Conditioning (HVAC) system,[3,6,7] which provides an indoor air environment in modern life, adsorption filters previously played an essential role in filtering harmful substances.[8] However, it needs to be substituted at fixed intervals due to contamination, which cannot meet future demand. Considering the requirement for blocking the transmission of airborne microorganisms and eliminating the residual biological contamination simultaneously, the electric method: electrostatic precipitation, and nonthermal plasma are

Received: May 30, 2024
Revised: July 9, 2024
Accepted: July 9, 2024
Published: August 13, 2024

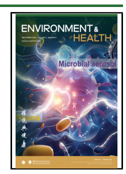

https://doi.org/10.1021/envhealth.4c00100
Environ. Health 2024, 2, 596−617

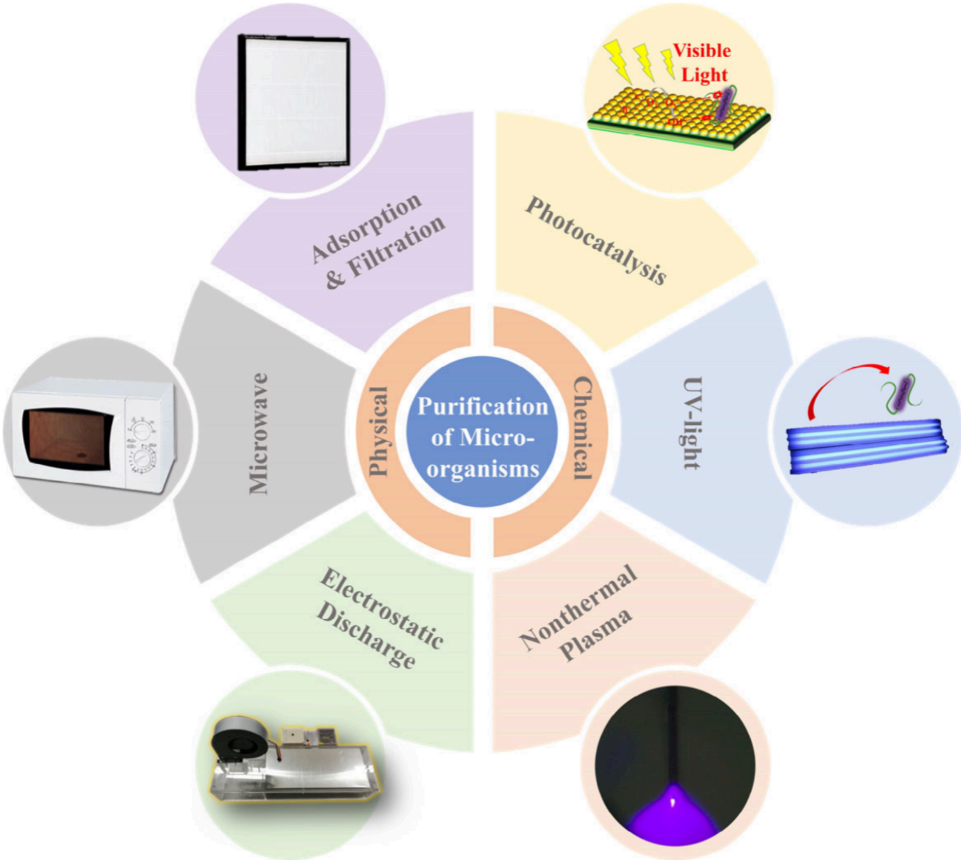

Figure 1. Methods for the Removal or Disinfection of pathogenic biological aerosols

more feasible. Compared to microwave,[9] UV-light,[10] and photocatalysis,[11−13] which is popularly adopted in static state sterilization, the electric method combining microbial aerosol collection with deactivation is more effective and feasible.[14] It effectively builds a clean and sanitary respiratory environment for human life.

Generally, microbial aerosols, such as bacteria and viruses, are minimal. For example, the diameter of the influenza virus is about 0.12 μm,[15] approximately 0.08−0.12 μm and 0.12−0.14 μm for the SARS virus and MERS virus,[16] respectively. Usually, microorganisms attach to the submicron particles or form microbial aerosols.[17] For instance, it is around 0.1−0.6 μm for mycoplasma pneumonia.[18] Since the characteristics of these pathogens' transmission in the air are similar to those of particulate matter, an electrostatic precipitator (ESP) is a perfect choice for removing fine particulate matter and microbial aerosols in the meantime. In the past few decades, electrostatic precipitation has proved effective for air purification due to its excellent performance, good economy and controllability, and high security.[19−22] The aerosol particle is first charged by corona discharge, aggregated by the agglomerator, and then moves to the electrode plate under the action of the electric field force and is finally captured. Simultaneously, the electric field also kills microbial aerosols.[23] In addition, the electrostatic precipitator can also produce ozone and negative air ions[24,25] that have a killing effect through lipid and protein peroxidation.[26] All of these fortes make electrostatic precipitation popular with engineers and researchers. From both research and application viewpoints, the efficient electrostatic precipitator applied in the HVAC should be qualified with the following characteristics: (1) High removal efficiency for submicron particles.[27] It was demonstrated that an electrostatic device has low trapping efficiency for submicron particles of this kind of microbial size level, especially at the range of 0.2 μm- 0.5 μm, which is caused by the dual effects of low charge and weak Brownian diffusion.[19,28,29] To remove the submicron airborne pathogenic aerosols efficiently, we should strengthen the entire process in the electrostatic device, especially the agglomeration process.[30] (2) Low re-entrainment particles at high gas velocity. Most research about electrostatic precipitation is currently accomplished at a gas velocity of 1 m/s. Furthermore, it was found that the increase in gas velocity would directly lead to a decrease in the collection efficiency.[31] By offline observation of the microstructure on the collection plate, researchers proposed that the agglomerated particles growing on the collection plate tend to form re-entrainment, which may be intensified with increasing gas velocity. Few researchers reported the in situ observation. Jin et al.[32] studied the agglomerated particles of chain structure on the collection plate at different moments by the microscope and attributed its formation to dipole−dipole force. Moreover, Zhu et al.[33−35] studied the dynamic evolution of particle chains at the electrode surface with a microscope and high-speed camera. It visually revealed that the re-entrainment in the ESP is related to the fracture of the particle chain. (3) Low emission of byproducts like ozone, etc. It is well-known that the ozone generated by corona discharge is a double-edged sword, which would cause severe environmental pollution and threats to respiratory health without control. Nevertheless, it is also a powerful oxidant for the oxidation and disinfection of airborne hazardous substances. Therefore, it is feasible to control ozone

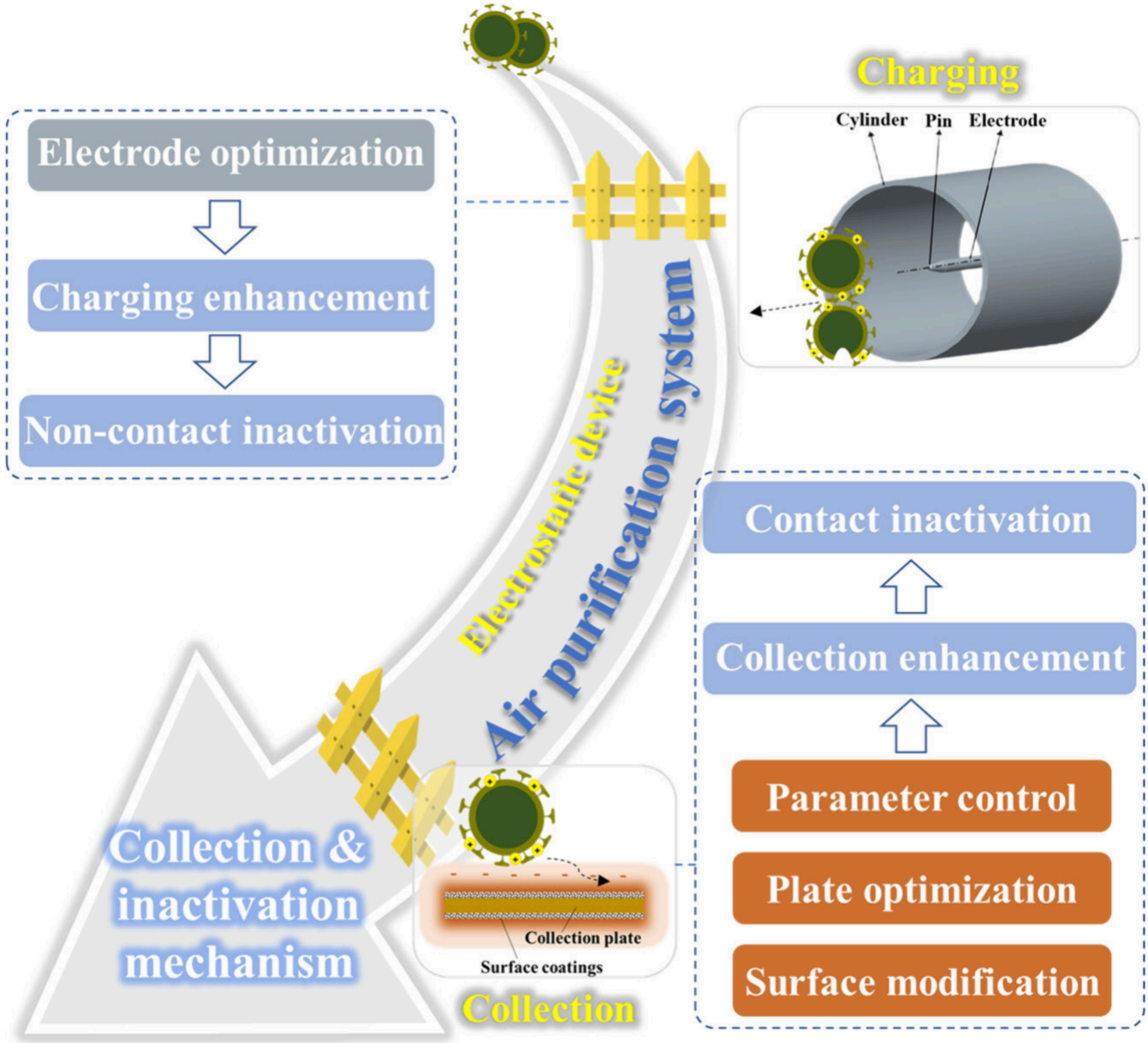

Figure 2. Mind map of the collection enhancement mechanism in public air purifying system.

production and simultaneously take full advantage of it to solve the problem.

On the other hand, despite these recent findings on the role of electrostatic precipitation in air purification, it still cannot meet the demands of efficiently removing multiple pollutants in different situations. As an emerging technology with outstanding purification ability, the nonthermal plasma method is attracting more and more attention. It usually produces abundant reactive species by discharge with direct current or alternating electric field based on the corona discharge (CD) or dielectric barrier discharge (DBD). It is usually generated at a higher electric field strength than the relatively mild discharge in electrostatic precipitation. The nonthermal plasma from discharge in gas is composed of electrons, free radicals, excited ions, and neutral atoms, which can further undergo oxidation reactions to generate reactive oxygen and nitrogen species (RONS) and excite photons (such as ultraviolet photons). The past decade has seen the rapid development of plasma in many fields, like VOCs,[36−38] NO_x,[39] and particle matter (PM).[40,41] More importantly, RONS can damage the surface proteins and gene chains of microorganisms, and the ultraviolet radiation generated by plasma is considered to have a sterilizing effect.[42−44] With the development of modern science, there has been thorough research about nonthermal plasma's physical and chemical principles.[45,46] However, in terms of the application, nonthermal plasma usually plays the role of ionizer[47,48] and particle collector,[49] which is far from satisfactory. The research about the novel and efficient application in removing airborne pathogenic microbial aerosols is unfolding. In brief, some crucial points need to be discussed and developed: (1) use security.[50] (2) coordination in the integrated system.[51] The former mainly refers to the high concentration byproducts and the operating parameters like applied AC voltage for DBD. In contrast, the latter is a scientific engineering problem: matching the plasma with other modules such as the power supply to form an integrated air purification system with high efficiency.

This paper first summarizes the primary mechanism for collecting and disinfecting pathogenic microbial aerosols by electrostatic methods and provides a comprehensive overview

https://doi.org/10.1021/envhealth.4c00100
Environ. Health 2024, 2, 596−617

Table 1. Summary of Examples for Collection Enhancement and Their Advantages and Disadvantages

Parts	Methods	Example	Advantages	Disadvantages	Reference
Charging	Electrode optimization	Corona discharge	Widely applicable	Small scale	54
		Dielectric barrier discharge	High efficiency	High cost	55
Collection	Parameter control	Collection length	Simple; controllable	Efficiency limitation	56
	Plate optimization	Baffle structure	High efficiency	Not easy to clean	57
	Surface modification	Dielectric-constant coatings	High efficiency; low ozone	Low handling capacity	58

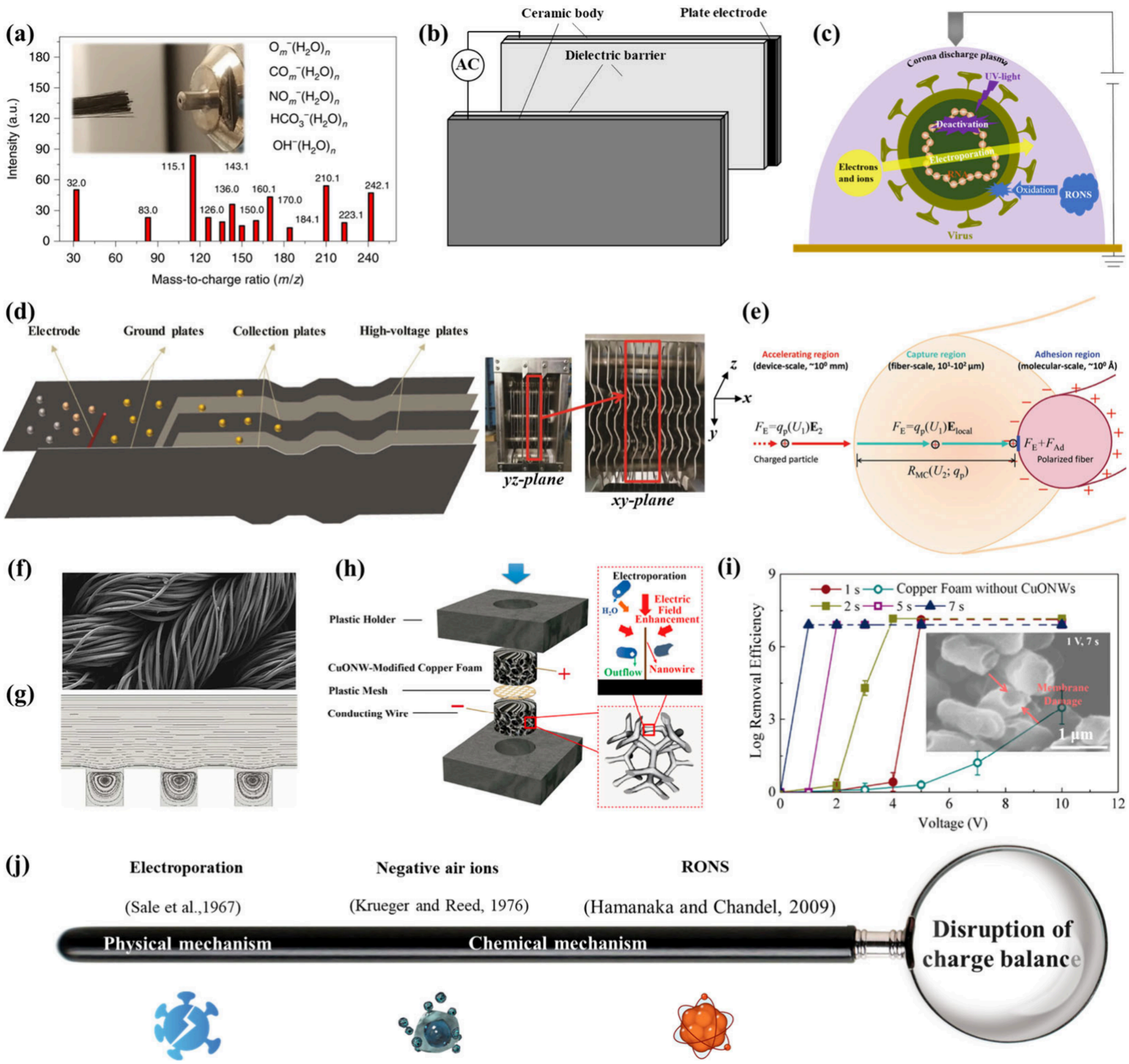

Figure 3. (a) identification of the NAI species generated at the TENG-actuated carbon fiber electrodes using mass spectrometry. Reproduced with permission from ref 24. Copyright 2020 Springer Nature; (b) schematic of the dielectric barrier discharge (DBD); (c) schematic of the deactivation of virus treated with corona discharge plasma; (d) 3D geometry model of the W-plate structure. Reproduced with permission from ref 57. Copyright 2020 Elsevier; (e) schematic of enhancing filtration efficiency of air coarse filter by electrostatic and adhesion effect in three regions. Reproduced with permission from ref 58. Copyright 2021 Wiley; (f) uneven topography of microbicidal fabric on the plate (SEM photograph at 363× magnification);[67] (g) Recirculating flow due to uneven topography simulated in OpenFOAM-7;[67] (h) three-dimensional schematic of the electroporation−disinfection cells (EDCs) that consist of copper oxide nanowire (CuONW)-modified copper foam electrodes;[68] (i) Removal efficiency of *E. coli* varied with applied voltage at different hydraulic retention times (HRTs) and SEM images of *E. coli* after a 1 V, 7 s treatment;[68] (j) timeline of the inactivation mechanism research about electrostatic method.

of the latest advances in physical and chemical mechanism research about collection reinforcement and deactivation. Besides, the frontiers in the mathematical modeling of migration and deactivation of pathogenic microbial aerosols are discussed in detail. Moreover, the novel research about constructing a comprehensive protection system for human health is discussed, especially the cooperative control of byproducts and purifying efficiency. Last but not least, we also have an outlook on future research after concluding the reported work. We hope this work can comprehensively summarize the advanced theories and application strategies of electrostatic aerosol purification methods, which will help develop efficient and safe integrated air purification technologies in the future.

2. ADVANCES IN COLLECTION AND INACTIVATION MECHANISM

For submicron aerosols at 0.2 μm - 0.5 μm diameter or even smaller, diffusion charging may be more critical. Moreover, it depends on the particle diameter, space charge density, particle residence time in the ionic region,[52] etc. Researchers separated the charging and trapping processes to improve the removal efficiency of submicron particles. They devised a two-stage electrostatic device to improve the charging process and restrain ionic wind generation.[53] The primary enhancement mechanism for the two-stage electrostatic device is shown in Figure 2. The detailed information is summarized in Table 1.

Next, the quotes and discussions would be conducted, aiming at the charger and collector module. The physical and chemical processes of purification are the leading research topic.

2.1. Charging

Throughout the process of particle removal, charging is the prerequisite. In terms of charger, in addition to directly enhancing the particle charge by increasing the applied voltage of the charger,[56] Yao et al.[59] studied the effect of discharge polarity on the collection of microorganisms. They found that a negative electric field was more effective than a positive electric field related to the high concentration of negative ions around the electrode. To meet the demand for abundant space charge, nonthermal plasma was usually employed for particle charging. Generally speaking, there are mainly two kinds of plasma generators: corona discharge and dielectric barrier discharge (DBD), determined by the discharge electrode-spike or plate electrodes, as shown in Figure 3(c) and Figure 3(b), respectively. The structural differences may directly determine the distinctions in the charging and collection of submicron aerosols.

Turning now to the corona discharge plasma, there are mainly two types of electrode structure, wire-plate (tubular) and spike-plate,[19] both of which break through the air and generate plasma by the extremely high electric field on the electrode surface with relatively low curvature. Researchers have adopted various optimizing works to promote the space charge density, like wire-plate structure,[28,54] and electrode lines[60] with spikes and double corona discharge precharger. The wire-plate structure is commonly employed to build the electrostatic precipitator, including charger and collector.[54,56,61,62] The corona discharge is uniform along the electrode wire. Instead, the spike-plate structure can generate a relatively more intense ionization zone at the electrode tip, ensuring sufficient ions and charges.[19] Another significant aspect is its excellent controllability and low power requirements, making it more suitable for charging and widely noticed by researchers. Our group recently proposed a multistage spike-tubular corona discharge strategy, which ensures a high removal efficiency of over 99% for submicron particles.[63] Besides, Liu et al.[64] improved spike-plate structure to a modified vertically focused electric field for efficient PM collection and sampling.

Having illustrated the advantage of corona discharge, we will now discuss the DBD plasma supplied by an alternating current. It is often used in large-scale applications due to its flexible structure and large areas of stable plasma generated between the two parallel plate electrodes covered by a dielectric layer. In addition to charging, the AC electric field between the electrode plates is favorable for particle aggregation.[30] Besides, Byeon et al.[55] found that the relatively higher voltage and lower frequency are beneficial for removing submicron particles by DBD. So it is crucial to balance efficiency and the operating cost of AC voltage. Moreover, it has been found that electrostatic devices with DBD serving as a charger would generate more positively charged particles than negatively charged ones.[65] While the latter helps induce the inactivation of microorganisms.[66] It indicates that DBD may not be very effective in directly inactivating microorganisms by negative ions.

Although there have been significant improvements by structural optimization, the flexibility and efficacy still need to be enhanced. Other supplementary means may be more feasible in the application. Di Natale et al.[52] applied the electrospray to improve the charging in a wet electrostatic scrubber (WES). Kettleson et al.[69] used soft X-rays to generate additional bipolar ions or direct photoionization to enhance charging. What is more, Guo et al.[24] developed a tribo-electrostatic negative air ion generator with extremely high removal efficiency for PM2.5, which provides an inspiring case for designing a highly efficient and straightforward air ion generator used to strengthen the charging and precipitation process of particles. It is safer and more feasible for public air purification systems than AC-supported chargers like DBD.

2.2. Collection

After the charging process, the following section will discuss the collection process. It is widely acknowledged that the parameter regulation of collectors plays an essential role in improving collection efficiency. Due to the difference in operating conditions, it is more feasible to realize collection enhancement by optimizing structure parameters. The collection efficiency of the two-stage structure is usually enhanced by adjusting the spacing distance between the electrode (plate) and plate, the collection length, etc.[54,56] It would help improve the electric field force on the particles and provide more deposition places for them. In addition, it is worth mentioning that designing a collector with a unique flow channel structure can also be an effective way to improve the ESP performance. Zhu et al.[57] found that using a baffle structure, shown in Figure 3(d), can effectively improve the flow characteristics of the airflow and increase the removal rate. Chang et al.[70] designed a perforated plate and showed that the turbulence caused by ion wind was used to optimize particle agglomeration and improve the removal efficiency by 12%.

Based on research on collector structure, modifying the collection plate with functional material coatings can also be a novel method for increasing the PM removal efficiency,[71,72] which gradually received some attention. It was claimed that the dielectric coating effectively reduces the breakdown risks and restrains the release of ozone. Moreover, Prof. Jinhan Mo's group[58] constructed electrostatically responsive filters with polydopamine coatings to capture charged particles by electrostatic and adhesion effect, which could realize a relatively high single-pass filtration efficiency of nearly 100% in 30 days. The enhancement is ascribed to the induced polarized electric field, as shown in Figure 3(e). It provides valuable means to develop high-efficiency electrostatic filters. Benefiting from the enhanced electrostatic force of the dual-zone electrostatically actuated filter, the capture efficiencies for *E. coli* (Gram-negative) and *Staphylococcus epidermidis* (Gram-positive) aerosols with diameters of 0.3−0.5 μm increased significantly from approximately 25.4% to 98.4% at a filtering velocity of 0.5 m/s, while maintaining air resistance at only 4.5 Pa.[73] Similarly, Sim et al.[74] demonstrated the outstanding filtration performance of an electrostatic air filter decorated with nanoparticles. More interestingly, Zhang et al.[75] constructed a filter of Schottky-junction material by loading TiO_2 particles on carbon nano fiber, which can improve the filtration efficiency of 0.3 μm particles from 61.59% to 92.98% with UV−vis light irradiation. It was attributed to the enhancement in long-range electric field force driven by the polarization field at the interfaces and surfaces. Such work provides some insights into improving the collection efficiency of submicron aerosols. When discussing the application of a collector with a plate structure, the filter mentioned above can also be employed. Phadke et al.[67,76] combined microbicidal fabric with a parallel plate, as shown in Figure 3(f) to efficiently capture and inactivate microbial aerosols, which benefited from the recirculating flow due to uneven topography (Figure 3(g)).

2.3. Inactivation

2.3.1. Physical Mechanism. Having discussed how to enhance collection efficiency, the section addresses the physical inactivation mechanism-electroporation. Electroporation was first researched in 1967, as shown in Figure 3(j). Here is a summary of the classical theories together with the latest findings with meaningful enlightenment.

In the 1960s, Sale et al.[77] examined the disruption of cytomembrane induced by the electric field, also called electroporation. It was deemed to cause the electrolyte and charged ions in the phospholipid bilayer to migrate, and the ion concentration on both sides of the membrane changed. Eventually, the permeability increases, which leads to the destruction of the pathogen structure and death.[23] Based on this, novel research about microbial disinfection has proliferated.

The past decade has seen the rapid development of structure innovation in traditional electrostatic devices for microbial aerosol disinfection. Building an appropriate electrode structure for discharge is the key to realizing efficient sterilization. It is worth mentioning that Prof. Xie's group[78,79] put forward "locally enhanced electric field treatment (LEEFT)", which refers to the novel electrode decorated with functional nanowires. It can arrive at a high electric field strength of about 10^7 V/m at the tips of nano wires with a low applied voltage (~1 V), which would result in the electroporation of microorganisms and is exceptionally effective for water disinfection.[80] The mechanism and results are shown in Figure 3(h, (i). It can be known that LEEFT can reach a high log removal efficiency of 7−8 in several seconds. The destruction of the membrane structure is also undeniable. Moreover, they also adopted in situ observation of the collection and inactivation process,[81] which sets a research example for analyzing the dynamic characteristics of microbial aerosol in an electric field. On this basis, Huo et al.[79] successfully combined it with a two-stage electrostatic device to collect and inactivate airborne pathogenic microbial aerosols, marking significant progress in electrostatic air purification.

Besides the electric field strength, discharge current can also be an induction faction to inhibit the growth of bioaerosols.[82,83] He et al.[82] developed a self-sustaining smart air filter (SSSAF) by sandwiching the PZT/PVDF membrane with two metal mesh to harness wind energy, ensuring effective suppression of bacterial growth without requiring extra power. Although the voltage on the membrane is only 4 V, the electric current of 700 nA could kill 96% of the original bacteria in 5 h. The SSSAF was meticulously designed to tap into the energy naturally present in the airflow used for filtration, ensuring a consistent and self-sustaining power source for the system.

2.3.2. Chemical Mechanism. Since Kreuger and Reed[66] confirmed that negative air ions had effective inactivation performance for microorganisms in the 1970s, there have been several tidal waves of study on it, either for science or engineering. Kellogg et al.[84] investigated the killing effect of negative ions on Staphylococcus Albus and found that O_2^- generated by corona discharge would be converted into H_2O_2 in the liquid medium, thus effectively killing bacteria. Nevertheless, Digel et al.[66] thought the ions sterilize the virus primarily by binding to the surface protein. Similarly, Badhe and Nipate[85] proposed a hypothesis that negative oxygen ion clusters $[O_2^-(H_2O)_n]$ and bicarbonate ions $[HCO_3^-]$ generated by oxygen ionizer can act on the spike protein of the COVID-19 virus and turn the environment of the lung into neutral or alkaline, which relieves the patient's symptoms and helps them recover. In addition to chemical reactions between ions and protein, electroporation was also regarded as one of the negative ions' most critical disinfection effects.[86]

Based on the basic theory of discharge, researchers have put forward various optimization works to improve the ionizing process and thus strengthen the inactivation of microorganisms, such as developing novel electrode material[79,87] and establishing novel electrode distribution,[79] etc. The most popular ionizer is tightly packed carbon fibers.[79,88]

However, little evidence has been found associating species of negative air ions with microbial inactivation performance in the 21st century. "NAIs" is a nebulous term, more of an application terminology. According to existing research and applications, ozone and NAIs go hand in hand when electrostatic precipitator works. Even more surprising, there is a strong synergistic effect between ozone and NAIs on the inactivation of microorganisms.[89] It can be seen that in earlier research researchers had to define the species produced by air ionizing as NAI due to the underdeveloped mass-spectrometric technique. Subsequently, with the development of substance diagnostic procedures, it is gradually superseded by reactive oxygen and nitrogen species (RONS). It can be seen from Figure 3(a) that O^-,O_2^-, O_3^-,O_4^-,O_2^-, CO_3^-, CO_4^-, NO_2^-, NO_3^-, OH^- and HCO_3^- combined with $(H_2O)_n$ ions were detected from the NAIs released by corona discharge in the air.[24] Besides, atomic oxygen (O), singlet oxygen ($^1O_2$), ozone (O_3), and nitric oxide (NO) also play essential roles in the disinfection of microorganisms by the electrostatic device.[90−95]

However, the inactivation mechanism of the specific active species and microorganisms is still not precise enough in the research field of NAIs. For example, what is the priority for reacting to different ROS under different working conditions? Fortunately, the effect of RONS on microbial inactivation has been studied in detail and precisely in recent years due to the development of nonthermal plasma. Then there is a specific inductive discussion of such problems.

Figure 3(c) shows the sterilization mechanism of plasma technology in which RONS dominates. Although the traditional electrostatic precipitation method can also provide a certain amount of reactive species, the relatively low ionization intensity still can not meet the demand for high-efficiency and broad-spectrum sterilization. Exactly, nonthermal plasma technology can meet the demand for high energy density under the same working conditions. It has become a future-oriented sterilization technology in the air, water, and food and has received extensive research attention. More importantly, it proves feasible to study the difference in the effect of various RONS on the microorganisms by regulating the discharge atmosphere and other operating parameters, which could also intensify the disinfection. It breaks through the limitation of electrostatic precipitation technology.

According to the research on the biological effects of reactive oxygen species, ROS with relatively low levels would positively influence activity. In comparison, ROS at high levels tends to cause irreversible damage to the microorganisms' DNA/protein/lipids and accelerate death.[96] As plasma came into scientists' view, more details about reactive species generated from discharge emerged.

According to existing time, species were classified into two subtypes: long-living and short-living species when applying nonthermal plasma. Concerning the former, ozone is one of the most noticeable species for its excellent oxidation susceptibility, which is a double-edged sword. Ozone has been a representative sanitizer for water disinfection.[97] There has been heated discussion about whether ozone can control airborne viruses, especially COVID-19.[98−101]

Since it has been demonstrated that ozone is adequate to deal with viral diseases like Ebola and HIV, Tizaoui[102] evaluated its inactivation performance for the COVID-19 virus by molecular modeling. Besides, Alimohammadi and Naderi[103] further concluded that coronavirus like COVID-19 is easily destroyed by ozone due to the oxidation of cysteine-containing sulfhydryl groups. Bayarri et al.[104] concluded that the ozone inactivation of the enveloped virus is due to the alternation generated by ozone, which destroys its membrane. In contrast, the nonenveloped virus is unknown now. More importantly, relative humidity (RH) is confirmed to be positively correlated with the disinfection effects of ozone to a certain extent, which is easier to ignore than other common conditions such as temperature, reaction time, ozone concentration, etc. Specifically, the optimal relative humidity exists between 70% and 90%.[104,105] The high RH condition favors the generation of more radicals than those with low RH.

In contrast to the widely known ozone, other reactive species may be more efficient. It has been demonstrated that the amount of active species required to inactivate the virus per unit number is 75−750 times the amount of ozone generated in the same plasma reactor.[106,107] After further discussion of the inactivation mechanism of other kinds of RONS, more previously unknown facts come into view. Ozone is widely known to the public for its brilliant stability and reliability in disinfection. However, the inactivation ability of $^1O_2$ proves to be better than that of the long-lived species.[108] The histidine residues would be oxidized during the inactivation process.[23] Moreover, it would also cause a shift in the molecular mass of the methionine residues. Besides, cysteine, tyrosine, tryptophan, and guanine would also react with $^1O_2$.[108] So the singlet oxygen is crucial for the disinfection of feline calicivirus[23,45,109] and bacteriophage T4.[108] Apart from chemical reactions, singlet oxygen can also induce protein cross-linking inside the capsid.[110] However, the other two main reactive oxygen species, ozone, and hydrogen peroxide play a secondary role in inactivating calicivirus,[45,23,111] MS2,[107] and adenovirus.[112] And the latter may be rare in the inactivation process of pathogenic microbial aerosols. The reactive nitrogen species are usually considered to be critical factors in research about feline calicivirus. The species of interest are $ONOO^-$[109] and ONOOH[45,99] (when in an acidic environment). The peroxynitrite derived from $ONOO^-$ has a strong ability for diffusion and oxidation, which leads to lipid peroxidation and destroys the cell wall.[113] At the same time, an acidic environment or even a weak acid environment has an inhibiting effect on the inactivation process.[114] It is worth mentioning that these results are obtained from the experiment in the liquid phase, and they may not be entirely suitable in the gaseous phase. When the inactivation of aerosols is discussed, humidity may be a crucial factor. Based on the discussion above, a conclusion can be drawn that short-lived RONS play a vital role in inactivation. Gao et al.[115] examined the inactivation enhancement of pathogenic microbial aerosols by subjectively increasing the concentration of short-lived species. They realized this by enhancing the electron energy and adjusting the airflow rate. The former is obtained by fast-rising time voltage pulses, considering the plasma chemistry.[116] At the same time, the latter may be simpler but not very effective due to the future demand for air purifiers with high purification capacity.

In our opinion, both objective and subjective factors need to be considered. For the environmental factors, the humidity should be reasonably controlled in this reason. Besides, the reactor's volume proportion of corona discharge must also be expanded to increase the interaction time between plasma and aerosols. As described below, modeling and simulation are essential for the accurate analysis and control of related parameters.

Besides the chemically active species generated by discharge, the surface functional groups of the collection media could also have a chemical effect on the disinfection of bioaerosols. The primary mechanism operates by leveraging the positive charge carried by the metal/organic ions adsorbed onto the bacteria's surface. When these positive ions approach the cell membrane, an electrostatic attraction arises due to the membrane's negative charge, resulting in a Coulombic gravitational force. This force facilitates the penetration of the cell wall, ultimately leading to the demise of the bacteria.[117,118]

This effect could be attributed to the interaction between positively charged amino groups and the bacteria, potentially disrupting the delicate equilibrium between bacterial cell wall synthesis and dissolution. Consequently, this disruption may lead to the leakage of intracellular components and ultimately result in bacterial cell death.[119,120] Based on it, Sun et al.[121] proposed a positively charged and chitosan-dipped air filter for

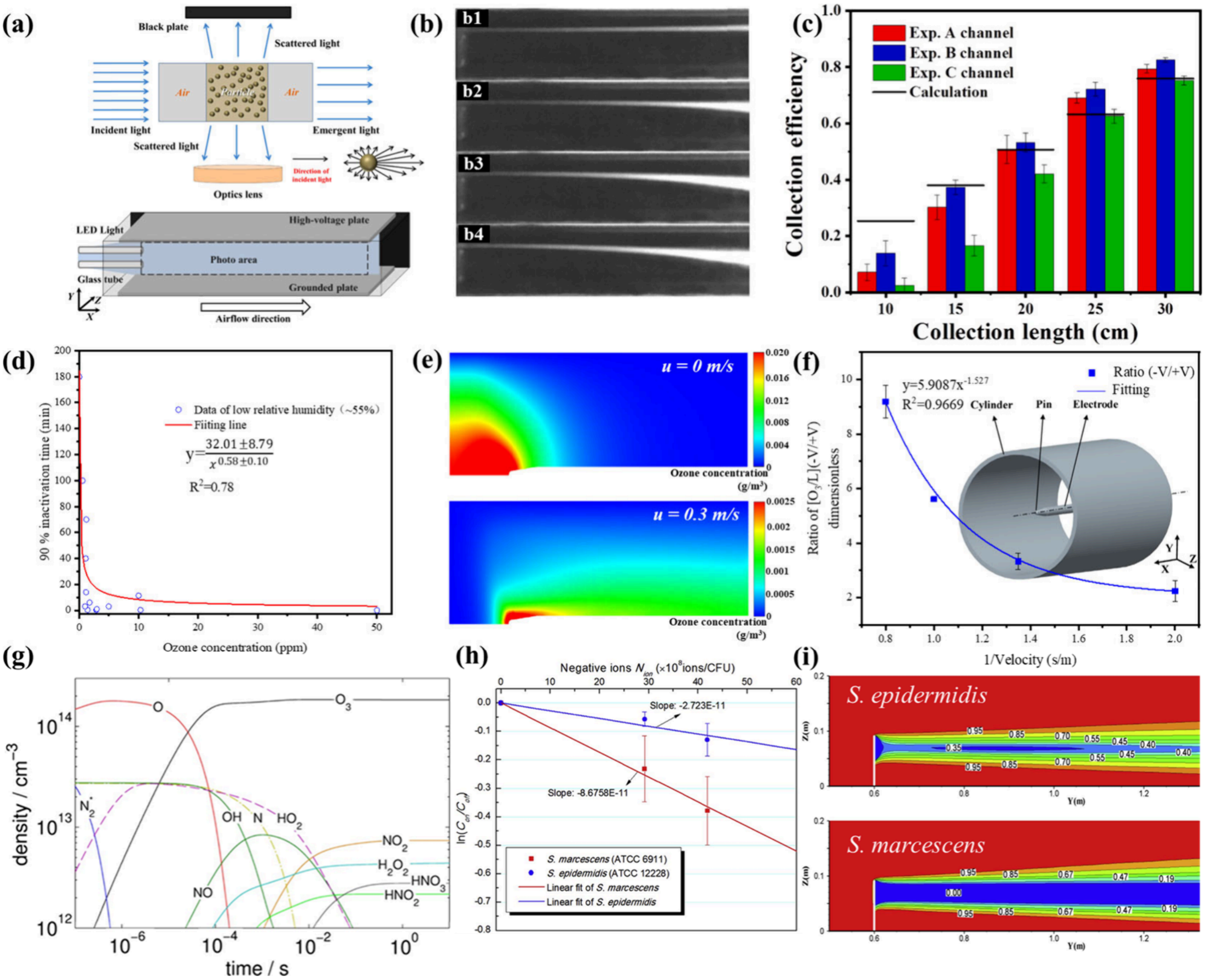

Figure 4. (a) Schematic of experimental investigation about the dynamic characteristic of submicrometer-scale aerosol in a high-voltage electric field by a visualization method; (b) visualization images of the particle motion at different working conditions: the charger of 1.0 kV and collector of (b1) 0, (b2) 1, (b3) 2, and (b4) 3 kV/cm; (c) collection efficiency comparison of the experiment results and the calculation value when the particle diameter was 0.25 μm (Electric field strength: 6 kV/cm, gas velocity: 4 m/s). Reproduced with permission from ref 130. Copyright 2021 Elsevier; (d) relation between ozone concentration and contact time in the process of microbial inactivation; (e) evolution process of ozone concentration of pin-cylinder discharge device under different gas velocities: u = 0, 0.3 m/s; (f) relation between the dimensionless parameter-ratio of $[O_3/L]$ (-V/+V) and the reciprocal of velocity. Reproduced with permission from ref 144. Copyright 2020 Elsevier; (g) reactive species density at different times. Reproduced with permission from ref 145. Copyright 2014 IOP; (h) susceptibility constant of *S. epidermidis* and *S. marcescens*; (i) distribution of *S. epidermidis* and *S. marcescens* in duct flow at X = 0.1 m. Reproduced with permission from ref 146. Copyright 2019 Elsevier.

the inactivation of airborne bioaerosols. It was proposed that the charged filter media's positive charges and the -NH_3^+ groups found on the chitosan-treated filter media have the potential to engage with negatively charged bacteria. This interaction leads to a disruption of the metabolic equilibrium of the bacterial cells, ultimately resulting in their inhibition.

Overall, it can be summarized that disruption of the charge balance induced by physical or chemical mechanisms results in the inactivation of microbial cells.

3. MODELING OF THE COLLECTION AND INACTIVATION PROCESS

Since being invented in 1907, electrostatic devices have been studied efficiently and extensively to remove airborne particulate pollutants. Over the past 100 years, there has been a significant increase in analytical theories and numerical models of particle collection by electrostatic devices.[122−124] In comparison, numerical research on inactivation by the electrostatic device has been conducted in recent years.[125,126] More advanced modeling and numerical simulation work will be presented next.

3.1. Collection

Generally, three types have been identified as potentially significant in the modeling research of electrostatic precipitation: (1) Efficiency model based on the classical Deutsch theories;[127] (2) Numerical method for solving the particle advection-diffusion equation;[128] (3) Optimization of the Lagrangian method.[129] Fundamental theories of charging and agglomeration are becoming more mature and perfect. However, few reports have concentrated on mathematical

https://doi.org/10.1021/envhealth.4c00100
Environ. Health 2024, 2, 596−617

Table 2. Summary of the Inactivation Performance of Ozone

Ozone Concentration (Ppm)	90% Inactivation Time (Min)	Relative Humidity	Viruses	Reference
0.05	180	35%	Herpes	132
10.33	0.3	55%	Ssdna,Ssrna,Dsdna, Enveloped Dsrna	106
1.23	70	55%	4 Phages	133
10	11.36	55%	Different Viruses	134
0.6	100	55%	Ssdna,Ssrna,Dsdna, Enveloped Dsrna	135
1.2	14	55%	Ssdna,Ssrna,Dsdna, Enveloped Dsrna	135
2.9	0.307			106
1.8	6	40%	Φx174 Her-036	136
1.43	0.307	55%	Φ6 Atcc 21781-B1	106
1.13	40	55%	Φ6 Her102	133
5	3	52%	Hepatitis A Hm175/18 F	137
28	60	40%	Herpes Simplex-1, Bc-Cdc	105
20	90	40%	Influenza A/Wsn/33 H1/N1	138
3	1	52%	Murine Norovirus-1 S99	137
1	3	52%	Murine Norovirus-1 S99	137
1.13	10	85%	Ms2 Her462	133
2.3	0.307	85%	Ms2 Atcc 15597- B1	106
0.23	70	85%	Murine Norovirus- 1 Pta-5935	133
3.5	0.307	85%	T7 Atcc 11303-B1	106
0.075	35	70	Φ X174	139
1.6	0.307	85%	Ms2 Atcc 15597-B1	106
1.13	40	85%	Φ6 Her102	133
20	18	80%	Influenza A/Wsn/33 H1/N1	138
50	40	80%	Influenza A/Wsn/33 H1/N1	15
20	90	80%	Influenza A/Wsn/33 H1/N1	36
20	18	80%	Murine Norovirus	140
5.25	30	99%	Sars-Cov-2	141
0.9	40	85%	Φx174 Atcc 13706-B1	106
100	180	85%	Theilers' Murine Encephalomyelitis Virus	142
1	60	70%	Sars-Cov-2	142
6	55	70%	Sars-Cov-2	143

models and simulation methods of migration and collection processes for pathogenic microbial aerosols in the electric field, which could be more macroscopic and valuable. Our group recently proposed a novel visualization method based on Mie scatterings, providing a new way to research aerosol dynamic characteristics in the electric field,[130] as shown in Figure 4(a, b). By analyzing the particle motion behavior in the electric field under various working conditions, we defined a dimensionless calculation formula for describing the relation between the collection efficiency (η) of aerosol particles and multiple parameters, shown as follows.

$$\eta = \frac{V_j q_p L_j}{3\pi\mu D^2 u_x d_p} \tag{1}$$

where V_j is the electrostatic potential of the collector (V), q_p is the particle charge number, L_j is the length of the grounded plate (m), μ is the viscosity coefficient of laminar flow (kg/(m·s)), D is the plate-to-plate spacing (m), u_x is the x-direction component of the gas velocity and the d_p is the particle diameter (m). This formula provides practical, theoretical support and a method for studying aerosol particles' motion dynamics and even microorganisms' migration and capture process in the electric field, as verified by the comparison of experimental value and calculated value shown in Figure 4(c).

3.2. Inactivation

As explained at the beginning of the section, it is clear that the modeling research of inactivation behavior is less developed than that of collection. In particular, the former is more complicated due to the coupling effect of ozone and other reactive species. We will discuss them step by step in the following.

In the application field of electrostatic methods for microorganism inactivation, ozone was the pioneer in the fight against the virus.[131] We concluded the performance of ozone disinfection as shown in Table 2. Furthermore, the relation between the 90% inactivation time and the ozone concentration at a relative humidity of about 55% was further analyzed in Figure 4(d), which shows an exponential relationship. In the region of the ozone concentration (0−3.19 ppm), the inactivation time decreased rapidly with ozone concentration. While at relatively high ozone concentrations, the promoting effect is not apparent, which may also cause secondary pollution. However, there is no general regularity for the inactivation performance at high relative humidity. Experimental results obtained at average relative humidity may be more instructive. Besides, Jahromi et al.[101] did a numerical simulation of the ozone distribution in an enclosed space. They put forward that it can help to find the appropriate location of the generator/fan for a high-efficiency disinfection process in a short time.

Moreover, a novel simulation method for forecasting the ozone distribution in the corona discharge process of the pin-cylinder electrostatic device has also been established,[144] verified by experiment. From Figure 4(e), it can be directly known that the gas velocity increase contributes to ozone's

https://doi.org/10.1021/envhealth.4c00100
Environ. Health 2024, 2, 596−617

Table 3. Comparison of Inactivation of Various Microorganisms under Non-Thermal Plasma (NTP) Treatments

Microorganism	Treatment characteristics	Log reductions reported	Reference
C. jejuni	Atmospheric pressure plasma jet (APPJ), argon (Ar) and ambient air	1.5−2.5	151
E. coli	DBD, ambient air	4−4.3	152
E. coli	Corona discharge plasma jet, Ar	∼ 4	153
E. coli	DBD, in package	4.5−6.0	154
E. coli, S. enterica	Diffuse coplanar surface barrier discharge (DCSBD), ambient air	5.9 and 5	155
E. coli, S. enterica, B. subtilis	DCSBD, ambient air	∼ 6.5, ∼ 6.5, ∼ 5	156
E. coli O157:H7, S. aureus, S. Typhimurium	Corona discharge plasma jet, dry air	4.5−5.0	157
L. monocytogenes, L. innocua	APPJ, ambient air and N_2	∼ 2.5	158
S. enterica; E. coli	Corona discharge plasma jet, ambient air	5.3, 5.5	159
S. Enteritidis	APPJ, ambient air	3.5−5	160
S. enterica serovar Enteritidis, E. coli O157:H7, L. monocytogenes	DBD, (Helium) He and moisture	3.1 ± 0.1, 1.4 ± 0.1, 1.1 ± 0.1,	161
B. amyloliquefaciens	DBD, ambient air	∼>8	162
B. subtilis	DCSBD, ambient air	∼2	156
B. subtilis var. niger	DBD, 22% O_2, 30% N_2, 40% CO_2 and 8% Ar	5−6	163
G. stearothermophilus	DBD, Ar	3	164
A. flavus, A. alternata, F. culmorun	DCSBD, ambient air	4.2, 3.2, 3.8	165
A. niger spores	SDBD, O_2, humidified compressed air, and humidified O_2	3−4	166
Z. rouxii	DBD, ambient air	∼5	167
Z. rouxii	APPJ, ambient air	2.4−6.85	168
F. calicivirus	DBD, ambient air	4.5	169
Murine Norovirus	APPJ, ambient air	3−7	170

dissipation. Besides, there is a linear relationship of high fit between the ozone concentration per unit current and the reciprocal velocity, which applies to both positive and negative polarity. Meanwhile, Figure 4(f) indicates that gas velocity affects the ozone concentration generated from different polarities, presented as a power function. This work efficiently provides the theoretical basis for constructing the numerical relationship between the operating parameters of the electrostatic device and the inactivation efficiency.

$$\frac{\partial C}{\partial t} + u_x\frac{\partial C}{\partial x} + u_y\frac{\partial C}{\partial y} + u_z\frac{\partial C}{\partial z} = \frac{\partial}{\partial x}\left(D_x\frac{\partial C}{\partial x}\right) + \frac{\partial}{\partial y}\left(D_y\frac{\partial C}{\partial y}\right) + \frac{\partial}{\partial z}\left(D_z\frac{\partial C}{\partial z}\right) + S(x, y, z, c, t) \tag{2}$$

Having discussed ozone, the following section will address the modeling of the effect of ions generated by discharge. For example, Kim et al.[145] tried to evaluate the numerical relation between the susceptibility constant[126] of *E. coli* and the concentration of air ions by the linear regression coefficient "*Z*". It represents the microbial effects of air ions with different polarities on *E. coli*, which indicates that positive ions may be more effective in the inactivation of *E. coli*. This conclusion contradicts what we know about the negative ions. Similar results were also obtained in the work of Nunayon et al.[146] They explained that microbial aerosols carrying negative charges are more easily deactivated by positive ions, although the concentration of negative ions is much higher than that of positive ions. In addition, Kang et al.[147] demonstrated the repulsive interaction between the textile of negative electric potential and SARS-CoV-2 aerosol carrying negative charges, which indicates that the assumption of Nunayon et al.[146] is plausible.

The inactivation behavior of air ions released by discharge cannot reflect the combined influence of plasma on the microorganisms. When discussing the intrinsic reaction dynamics of the microbial aerosol inactivation process, survival curves may be one of the most simple and effective means. Two different equation models have been adopted to characterize the inactivation dynamics of three kinds of microorganisms treated with a plasma jet.[148−150] In particular, the survival curves of the vegetative cells of *Bacillus subtilis* and *E. coli* are based on the same equation.

$$\log_{10} s(t) = \log_{10}\left[\frac{N(t)}{N_0}\right] = -bt^n \tag{4}$$

For the vegetative cells of *Bacillus subtilis*, $n > 1$; while for the *E. coli*, $n < 1$. However, the equation used for *Murine norovirus* is a fractional function shown below.

$$\log_{10} s(t) = -\frac{k_3 t}{k_4 + t} \tag{5}$$

The reaction model was built to better apply electrostatic methods in pathogenic microbial aerosols' inactivation. Combining numerical simulation with experimental research for engineering applications and research is better. The detailed data of inactivation dynamics under nonthermal plasma (NTP) treatments are shown in Table 3. It is demonstrated that nonthermal plasma (NTP) treatments pose significant potential for inactivating a wide range of microorganisms. The effectiveness is influenced by the type of plasma treatment, the gaseous environment, and the specific microorganism. DBD and DCSBD methods in ambient air tend to achieve higher log reductions, especially for bacterial pathogens.

For characterizing the time scale of active species in the corona discharge process, Schmidt-Bleker et al. used COMSOL combined with Fourier transform infrared (FTIR)

https://doi.org/10.1021/envhealth.4c00100
Environ. Health 2024, 2, 596−617

to establish relevant models.[171] On the one hand, they employed FTIR spectroscopy to measure the absolute value of ozone and NO_2 generated from the plasma jet. At the same time, COMSOL was applied to determine the correct time scale for the species generation. The results are shown in Figure 4(g), which helps study the change of species and control the reaction atmosphere to alter the selectivity of species evolution.

Furthermore, numerical simulation was applied to explain the dynamic inactivation characteristic, mainly based on commercial computational fluid dynamics (CFD) software. For instance, Zhou et al.[172] adopted numerical simulation to study the microbial aerosol disinfection process in the air duct equipped with corona discharge plasma. They innovatively put forward a new continuity equation employed in calculating the change of the bacteria concentration in the air duct, which is as follows.

$$\frac{\partial C_i}{\partial t} + \nabla\cdot[(\vec{u} + \nu_s)C_i] = \nabla\cdot[(D + \varepsilon_p)\nabla C_i] - A\rho C_i \quad (3)$$

where A is the disinfection coefficient (susceptibility) ($m^3/(C \times s)$). By verifying the experiment, they set up the relation between the susceptibility constant and the concentration of negative air ions. The relevant results are presented in Figure 4(h). Moreover, the contour of the bacteria concentration in the air duct is shown in Figure 4(i), which provides valuable information for predicting the disinfection of electrostatic devices in engineering. Based on it, Feng et al.[173] put forward a more specific numerical method considering the synergistic effects of the electric field, electrohydrodynamic flow, and biological disinfection to comprehensively judge the microbial aerosol inactivation process in the air conduct. They optimized the traditional electrostatic device to an "electrostatic disinfector" (ESD) composed of an electrostatic device and filter, which is more feasible in application than a single electrostatic device or filter.

Until now, enhanced mechanisms and related numerical modeling research about airborne pathogenic microbial aerosols' collection and inactivation processes have been extensively expounded. The purposes of these works are intended to pave the way for building a reliable health protection system, which is the focus of the next section.

3.3. Model Validation and Details

Modeling and simulation of airborne aerosol disinfection involve understanding the behavior of aerosols in an airspace and evaluating the effectiveness of disinfection methods. Key factors include aerosols' physical and chemical properties, environmental conditions, and disinfection mechanisms.[6,174−180]

Aerosol dynamics play a crucial role in the simulation.[178] Aerosols range from nanometers to micrometers in size, and this size distribution affects their sedimentation, evaporation, and interaction with disinfectants. The primary transport mechanisms for aerosols include advection (air currents), diffusion (Brownnian motion), and sedimentation (gravitational settling).

Additionally, ventilation and airflow are crucial in determining the distribution and dilution of aerosols within a space, playing a significant role in controlling the spread of infectious particles like viruses and bacteria.[181] The mechanisms involved include natural ventilation through windows and doors, which allows outdoor air to dilute indoor contaminants, and the stack effect,[182] where warm air rises and escapes through higher openings while cooler air enters from lower levels. Mechanical ventilation via HVAC systems circulates and filters the air, while exhaust and supply fans manage air removal and introduction.[183] Hybrid systems combine both methods for the optimal air quality. Key influencing factors include the air exchange rate (measured in air changes per hour (ACH)) and ventilation rate, which dictate how frequently indoor air is replaced with outdoor air. Airflow patterns, such as displacement ventilation (introducing air at floor level and extracting it at ceiling level) and mixing ventilation (distributing air evenly), also impact aerosol removal efficiency.[184] Filtration systems, particularly HEPA filters and those with high MERV ratings, capture fine particles and enhance air quality.[185] Room design and occupancy affect aerosol concentration, with larger spaces diluting aerosols more effectively and higher occupancy levels necessitating increased ventilation.[186] Environmental factors like temperature, humidity, and outdoor air quality further influence aerosol behavior.[187] Specific examples illustrate these principles: healthcare settings use negative pressure rooms and high ACH in operating rooms to prevent infection spread; classrooms and offices improve ventilation and use air cleaners to reduce respiratory infection risks; public transportation employs advanced HVAC systems for filtration and directional airflow; and residential buildings benefit from regular use of exhaust fans and natural ventilation. Optimizing these factors can significantly reduce infectious particle concentrations and improve the overall air quality.

Disinfection mechanisms are another vital component.[172] Chemical disinfectants interact with aerosolized pathogens, and their effectiveness is influenced by the concentration, contact time, and reactivity. For the disinfection mechanisms of electrostatic plasma methods, its effectiveness depends on factors such as current intensity and electric field strength.

Computational Fluid Dynamics (CFD) is extensively used to simulate fluid behavior and interactions, which proves particularly useful for predicting aerosol dispersion, deposition, and transport in various environments. This capability is critical in fields such as environmental engineering, industrial hygiene, and healthcare. Several CFD techniques are utilized in aerosol simulations, each suited for specific scenarios. Direct Numerical Simulation (DNS) is highly detailed but computationally expensive, suitable for small-scale studies requiring high resolution.[188] Large Eddy Simulation (LES) balances detail and computational demand by resolving large-scale turbulence and modeling smaller scales, making it apt for urban dispersion studies.[189] Reynolds-Averaged Navier−Stokes (RANS) offers efficiency for steady-state and mean-flow analyses through turbulence models like k-ε or k-ω but may lack detail for transient phenomena.[190] The Discrete Phase Model (DPM) tracks individual aerosol particles within the fluid phase, ideal for HVAC systems and pollutant dispersion studies.[191] The Eulerian-Lagrangian approach, combining Eulerian treatment for the fluid and Lagrangian treatment for particles, provides detailed tracking but at a high computational cost. Accurate CFD simulations require careful parameter settings.[192] Domain size should encompass all relevant interaction areas with mesh quality adjusted to balance accuracy and computational load. Boundary conditions must accurately represent inlets, outlets, and walls, while turbulence models should be chosen based on flow characteristics, with constants adjusted based on validation data. Particle properties, including size distribution, density, and shape, must be defined

https://doi.org/10.1021/envhealth.4c00100
Environ. Health 2024, 2, 596−617

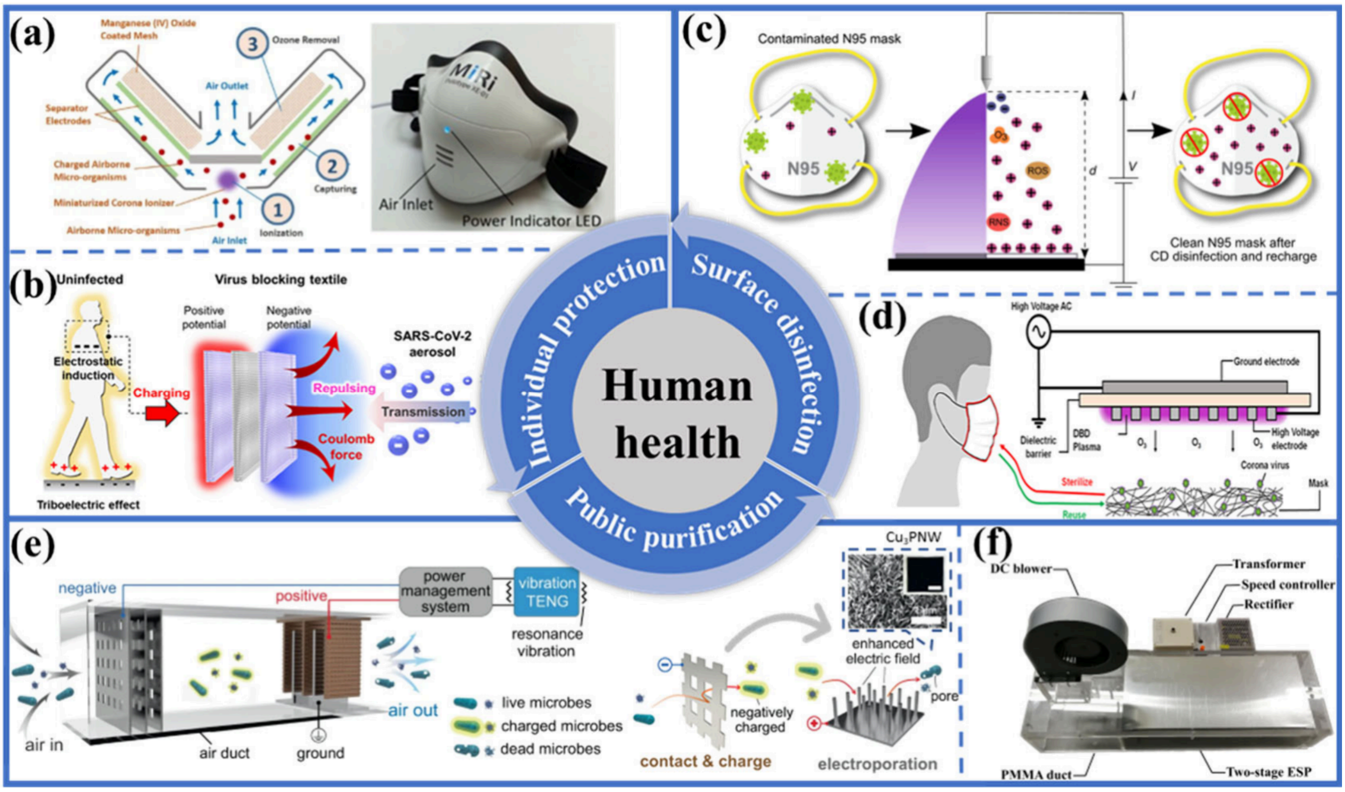

Figure 5. (a) Top-view operational schematic of structure design of microorganism-ionizing respirator, photo of the commercial prototype with its custom facepiece and power indicator LED light and the analytic particle removal efficiency; Reproduced with permission from reference 195. Copyright 2018 Elsevier. (b) concept of virus-blocking textile (VBT) that repulses SARS-CoV-2 aerosols using Coulomb forces. Reproduced with permission from reference 147. Copyright 2022 Elsevier; (c) Disinfection of contaminated N95 mask with corona discharge;[193] (d) schematic diagram describing the disinfection of a facemask by the ozone generated from a DBD plasma generator;[194] (e) schematics of the resonance-vibration-driven (RV)-disinfection system in an air duct[79] and (f) photo of the integrated electrostatic device. Reproduced with permission from reference 56 ; Copyright 2020 Elsevier.

to reflect realistic behavior. Time step size should capture transient phenomena without excessive computational demand, and convergence criteria must be stringent to ensure accurate results. Interpreting CFD results involves validation and verification to ensure the accuracy. Verification confirms numerical methods, while validation compares results with experimental data. Postprocessing includes flow visualization, particle tracking, and statistical analysis to derive meaningful insights. Sensitivity analysis assesses the impact of parameter variations, and uncertainty quantification evaluates the confidence in the results. Practical applications range from indoor air quality assessment to urban pollution studies, providing actionable insights for design optimization and health risk assessments.

CFD is a powerful tool for aerosol simulations, offering detailed insights into fluid-particle interactions. The appropriate choice of simulation methods, parameter settings, and careful result interpretation is crucial for accuracy. Future advancements may involve integrating machine learning to enhance predictive capabilities and reduce computational costs.

Moreover, kinetic models describe the interactions between disinfectants and pathogens, utilizing reaction kinetics and dose−response curves to predict pathogen inactivation rates.[174] Validation methods include comparing simulation results with experimental data to ensure accuracy. Sensitivity analysis evaluates the influence of various parameters on model outcomes, and uncertainty quantification addresses uncertainties in the model inputs and parameters.

For model validation, experimental comparisons are made through chamber studies in controlled environments and field studies in real-world settings. Statistical methods, such as calculating mean absolute error (MAE), root-mean-square error (RMSE), and R-squared values, quantify model accuracy, while confidence intervals assess the reliability of the predictions. To ensure robustness, a scenario analysis validates the model across different environmental conditions, aerosol types, and disinfection methods.

Key considerations include justifying model assumptions such as uniform aerosol distribution, ensuring scalability to handle different scales from small rooms to large buildings, and deriving practical implications for improving ventilation systems, disinfection protocols, and public health policies.

In conclusion, the effective simulation of airborne aerosol disinfection requires comprehensive modeling of aerosol dynamics, environmental conditions, and disinfection mechanisms. Rigorous validation through experimental comparisons and statistical analysis ensures the reliability of the model, aiding in the design and optimization of disinfection strategies in various settings.

https://doi.org/10.1021/envhealth.4c00100
Environ. Health 2024, 2, 596−617

Table 4. Comparison of Electrical Energy Per Order (E_{EO}) Values on Different Air Disinfection Technologies

Disinfection technologies	Electrode material	Bacteria/Virus	E_{EO} ($kWh \cdot m^{-3} \cdot order^{-1}$)	ref.
Electrostatic assisted catalysis	Mixed metal oxide ($Ti/IrO_2 + TaO_2$)	*E. coli*	2.4×10^{-4}	205
	N/A	*E. coli*	1.0×10^{-3} to 2.0×10^{-4}	206
	$Ag-Co_3O_4$	*E. coli*	1.2×10^{-4}	207
	Laser-induced graphene	T4 bacteriophage	3×10^{-4}	208
Electrostatic precipitation	PET fiber	*E. coli* and *S. epidermidis*	2.75×10^{-5}	73
	$Cu(OH)_2$NW-Cu	*Pseudomonas syringae* and *Phi6*	0.85; 4.70×10^{-2}	209
	MnO mesh coated with MnO_2	*E. coli*	8×10^{-4}	210
	Copper-clad plates	*P. fluorescens*	1.2×10^{-4}	59
	Copper-clad plates	*B. subtilis var. niger* bacteria	6.5×10^{-4}	59
	N/A	*E. coli*	4.4×10^{-4}	211
	Cu_3PNW-Cu	MS2	2×10^{-4}	79
Plasma	N/A	*E. coli*	1.90×10^{-2}	212
	N/A	*Porcine reproductive* and respiratory syndrome virus	2.11×10^{-2}	213
	TiO_2/Cu^{2+}@perlite	*E. coli*	1.2×10^{-2}	214
	N/A	*E. coli*	7.18×10^{-2}	47
	N/A	*S. epidermidis*	6.25×10^{-2}	47

4. HOTSPOTS IN THE APPLICATION

4.1. Comprehensive Protection System for Human Health

For decades, researchers around the globe have been refining the electrostatic purification method to create superior purification systems for healthier living environments. The section examines three key applied research areas aimed at eliminating airborne pathogenic microbial aerosols: personal protection, public purification, and surface disinfection.

As far as individual protection is concerned, a face mask plays the most critical role. Park et al.[195] miniaturized the ESP and made a microbial ionization respiration mask, reducing respiratory resistance compared to traditional face masks, as shown in Figure 5(a). It has embedded catalytic fiber, ensuring the ozone's ultralow emission. The result of the purification test stated that the mask equipped with an electrostatic device could remove 0.5 μm particles at a gas flow of 10 L/min, which is feasible to intercept the transmission of submicrometer microbial aerosols. What is even more interesting is that Kang et al.[147] developed a novel virus-blocking textile (VBT) to repulse SARS-CoV-2 aerosols with Coulomb forces. They demonstrated that SARS-CoV-2 carries negative charges and harnesses the triboelectric effect from the human body to power the VBT, continuously maintaining a negative electrical potential continuously. This mechanism successfully blocked 99.95% of the virus in the experiments. The schematic of this process is shown in Figure 5(b). These findings offer valuable insights for developing portable personal barriers to protect humans from pathogenic aerosols.

In addition to removable personal air purifiers, integrated purification systems have garnered significant attention from researchers. As discussed in Section 2, optimizing electrode structures effectively enhances particle removal. However, the design of an integrated system is crucial when applying electrostatic devices for indoor purification. For instance, the development and coordination of the power supply with the electrostatic device are key to ensuring efficient and sustainable operation of the entire system. Huo et al.[79] developed a novel two-stage electrostatic device with a collection plate modified with Cu_3P nanowire, as shown in Figure 5(e). The Cu_3P nanowire dense array structure introduced in the conventional static apparatus improves the local electric field intensity in the collecting region up to 3×10^8 V/m. The design concept can also be verified in standard ion generators made of carbon fibers.[24] It has been developed an integrated electrostatic precipitator of the application level.[56] The details about it are presented in Figure 5(f). It was composed of a power supply module, a charging module, a collection module, and a fan module, of which the entire volume is about 0.00298 m^3. In addition to the structure design, the application of the power supply system is also very significant for the large-scale promotion of the purifying device, such as application in the office building, etc. Direct current power may be one of the best choices for the future development of electrostatic air purifiers. It can be compatible with various novel energy systems like solar power and triboelectrostatic nanogenerator.[79] One significant issue with electrostatic charging is the limited lifespan of the charging pins. It greatly affects the performance and practical application of electrostatic plasma methods. To address the problem, Gao et al.[196] placed the carbon brush ionizer in a cup holder with shielding air pumped in, protecting it from corrosion and contamination by dust. Additionally, the charger mentioned above was combined with a foldable PET collector,[197] achieving an average efficiency of 95.4% for 0.3−0.5 μm particles over 25 days. They also compared the ionic concentration of a metal pin, cascaded metal pin, and cascaded carbon brush using a commercial air ion detector, underscoring the exceptional air ion generation performance.

In the epidemic era, in addition to blocking the spread of viruses in the air, attention should also be paid to the disinfection and cleaning of potential virus pollutants, such as facemasks,[198,199] food,[200] and water,[46,201] etc. KS Narayanan et al.[193] employed corona discharge to sterilize the contaminated N95 mask, which could easily reach a log reduction of 2−3 against *E. coli* in about 7.5 min, as shown in Figure 5(c). Besides, the surface charge density of the mask could be retained at a higher level than a new one for about 5 days after being treated with corona discharge, ensuring their safe reuse. In addition to disinfection by direct contact, Lee et al.[194] sterilized coronaviruses (HcoV-229E) contaminated facemasks by the ozone generated from a DBD plasma generator, as shown in Figure 5(d). The high ozone concentration (120 ppm) made the virus lose its infectivity with a 4-log reduction with no damage to the mask's structure and function. Besides, there was no leftover ozone in the mask after being treated.

https://doi.org/10.1021/envhealth.4c00100
Environ. Health 2024, 2, 596−617

Moreover, plasma has also been successfully employed in daily diet disinfection. Hosseini et al.[202] studied the influence of cold plasma on sour cherry juice. It was found that plasma has an outstanding inactivation ability for *E. coli*. Nevertheless, it only had mild disruption of the total anthocyanin content (TAC) and vitamin C, which preserved the quality of the juice as much as possible. Besides, Tu et al.[203] employed a pair of nickel foam electrodes to inactivate the Na_2CO_3 electrolyte containing the SARS-CoV-2 virus, which realized efficient and rapid wastewater treatment.

Table 4 summarizes the electrical energy per order (E_{EO})[204] values for different air disinfection technologies, focusing on various electrode materials and their efficacy against other bacteria and viruses. The E_{EO} values indicate the energy efficiency of each technology, with lower values representing more efficient disinfection processes.

Electrostatic-assisted catalysis technologies using mixed metal oxide (Ti/IrO_2 + TaO_2) showed an E_{EO} value of 2.4 $\times 10^{-4}$ kWh·m^{-3}·order^{-1} against *E. coli*. Other studies have shown a range of E_{EO} values from 1.0×10^{-3} to 2.0×10^{-4} kWh·m^{-3}·order^{-1} with Ag−Co_3O_4 demonstrating a particularly efficient E_{EO} of 1.2×10^{-4}. Laser-induced graphene also presented a moderate efficiency against the T4 bacteriophage at 3×10^{-4}. Technologies using electrostatic precipitation, such as PET fiber, achieved highly efficient disinfection with an E_{EO} of 2.75×10^{-5} against *E. coli* and *S. epidermidis*. Other materials like $Cu(OH)_2$NW-Cu had variable E_{EO} values of 0.85 and 4.7×10^{-2} when tested against *Pseudomonas syringae* and *Phi6*, respectively. Plasma disinfection technologies exhibited relatively higher E_{EO} values. For instance, disinfection of *E. coli* had an E_{EO} of 1.9×10^{-2}, while the value for the porcine reproductive and respiratory syndrome virus was slightly higher at 2.11×10^{-2}. TiO_2/Cu^{2+}@perlite showed an intermediate efficiency with an E_{EO} of 1.2×10^{-2} against *E. coli*.

The findings align with existing literature, highlighting the efficiency of various disinfection technologies regarding E_{EO} values. Studies have consistently shown that mixed metal oxides and copper-based materials are highly effective for air disinfection due to their antimicrobial properties. The efficiency of electrostatic precipitation is particularly noteworthy, as it often outperforms other methods in energy efficiency. For instance, it was found that copper-coated electrodes could achieve similar low E_{EO} values for airborne bacterial disinfection. Additionally, studies on plasma technology often report higher E_{EO} values, which is corroborated by the table's findings, reflecting the trade-off between efficacy and energy consumption in plasma-based disinfection.

The practical implications of these findings are significant for industries and healthcare facilities looking to optimize their air disinfection processes. Technologies with lower E_{EO} values are more energy-efficient and can reduce operational costs. For example, electrostatic precipitation with PET fibers could be highly beneficial in hospital settings to ensure efficient disinfection with minimal energy expenditure. Furthermore, the choice of the electrode material can be critical. Mixed metal oxides and copper-based materials offer robust solutions for bacterial and viral disinfection and can be implemented in air filtration systems in public spaces to enhance air quality and reduce the transmission of infectious diseases.

The analysis of E_{EO} values for different air disinfection technologies underscores the importance of material choice and technology type in achieving energy-efficient disinfection. While electrostatic precipitation and certain electrostatic-assisted catalysis technologies show promise, plasma technologies still face challenges with higher energy consumption. Future research should focus on standardizing test conditions, expanding the range of tested microorganisms, and evaluating these technologies' long-term viability and economic aspects to fully realize their potential in practical applications.

4.2. Coordination between Byproducts Controlling and Efficiency Enhancement

Balancing removal efficiency with byproduct management, such as ozone, is essential throughout the application of the electrostatic method in air purification. As public awareness of air health rises, electrostatic air purifiers have become common in many households. However, the formation of byproducts, particularly ozone, remains an inevitable aspect of their operation. Although it can induce an adaptive reaction capable of reducing endogenous oxidative stress, it may help fight the damage to lung tissues caused by COVID-19.[100,215] There is a common saying in China that "as long as it is medicine, it has toxic components." In detail, long-term exposure to low-concentration ozone (<0.05 ppm) can lead to a decline in cardiopulmonary function.[216] It is especially prohibited from being used on pregnant women and patients.[98] Researchers have put forward various routes to solve the potential menace of ozone from the traditional electrostatic air purifier, such as catalytic removal,[217−219] discharge and structure optimization,[220] etc. To address the problem, three primary solutions can be identified: (1) Pretreatment, which reduces byproduct formation by adjusting the discharge environment and electrode structure; (2) Process control, which optimizes operating parameters of the discharge reactor to achieve high efficiency with minimal pollution release; and (3) Post-treatment, which involves combining the electrostatic device with a catalyst, a common method in the application of electrostatic devices. The following sections explore the advancements in these areas.

Ultimately, we should optimize the structure to reduce ozone emissions as much as possible without the help of other systems. Structural characteristics and operating parameters should be considered for optimizing electrostatic devices, such as electrode (material, size, and appearance), current density, applied voltage, polarity, etc.[221,222] In detail, electrode structure and discharge environment are included in the pretreatment, which prepares necessary conditions for generating the electrostatic field. Many researchers focused on its optimization because corona discharge is generated from the discharge electrode. Unfortunately, the metallic material seems to have little effect on ozone emission.[220] In contrast, carbon-based materials such as carbon fiber and carbon nanotubes[125,223−225] significantly inhibit ozone production, usually applied in the ionizer. Ye et al.[226] deposited carbon nanotubes on the needle electrode, resulting in zero ozone emission in the corona discharge. Simultaneously, decreasing the electrode diameter favors the control of ozone generation.[222] It has been tested by Boelter and Davidson[222] that corona discharge with negative polarity generated more ozone than that of positive polarity in the charger due to the difference in the space charge density, area of discharge region, and even the gas temperature. It is also worth mentioning that relative humidity (RH), temperature, and electrode contamination could influence ozone concentration.[221−223,227,228] Undoubtedly, there is a negative correlation between temper-

https://doi.org/10.1021/envhealth.4c00100
Environ. Health 2024, 2, 596−617

ature and ozone concentration,[228,229] while it is unclear for the relative humidity (RH).[221,222,228,230] Simultaneously, maintaining the cleanliness of the electrodes helps reduce ozone emissions.[227,230]

Besides, electrostatic characteristics, especially the current density, also play essential roles in generating ozone.[221,222,229] Our group has achieved relatively comprehensive research work and put forward the "ozone-efficiency two-factor criterion" based on regulating the electric field inside the charger and collector.[56,144] Specifically, it is more beneficial to enhance the electric field strength of the collector in controlling ozone emission and achieving high collection efficiency rather than simply increasing the charger's current.[56] Another significant aspect of process control is gas velocity, which determines the handling capacity. As shown in Figure 9, removal efficiency and ozone release are influenced by gas velocity and output power simultaneously,[56,144] which offers a "trade-off" relationship. The relationship between ozone concentration and independent variables and the comprehensive evaluation standard considering efficiency-ozone double factors is being constantly improved to optimize the structure design and working conditions of two-stage ESPs.

For post-treatment, researchers have adopted abundant studies. We believed that plasma-coupled catalysis would also be a promising method for overcoming this dilemma. On the one hand, catalytic technology effectively helps solve the problem of ozone escape, which guarantees environmental safety. Prof. Jinhan Mo's group[64,73,196,197,231] has done extensive research in the field of application research about cooperative control of PM removal efficiency and ozone emission. They developed surface coatings on electrostatically responsive filters to enhance the polarization electric field, while simultaneously eliminating ozone through catalytic effects. Future advancements in electrostatic air purifiers should focus on achieving high removal efficiency with ultralow byproduct emissions. Additionally, during the operation of an electrostatic device, less-oxidized VOCs, such as carbonyls and carboxylic acids, may form from reactions between ozone and terpenes.[232−234] However, there is also a study indicating that bipolar ionization devices work without ozone generation but produce more VOCs.[235] It was explained that the ionization energies of the commercial device are <12.07 eV[236] in that work, which does not meet the demand for the ionization of oxygen (O_2). However, in the process of corona discharge, VOCs would also be charged, just like particulate matter. The charging and removal of VOCs may induce many reactions between various organic molecules and the atmosphere, generating more uncharged novel products that could not be removed simply.[235] Thus, the concentration of VOCs is too high to be cleared by the ionizer. Therefore, the assistance of a catalyst is essential for the application of electrostatic devices.

Based on the fundamental strategies, various coordination modes have been put forward, such as the "ZeBox", which combines the nonionizing electric field and microbicidal materials in the parallel plate.[67,76]

5. CONCLUSION AND OUTLOOK

The electrostatic air purification method, either electrostatic precipitation or plasma, is the most promising solution to remove airborne pathogenic aerosols. This review presents a complete and detailed overview of highly efficient and sustainable electrostatic air purification methods, which assists researchers in learning state-of-the-art relevant novel electrostatic purifying technologies. Herein, some summaries of electric air purification research and innovative equipment design strategies for purification devices can be drawn as follows:

(1) To effectively remove submicron aerosols, it is helpful to optimize the charging and collection process by adding efficient chargers like carbon fiber ionizers and improving the electrode structure to enhance the local electric field strength. Certainly, agglomeration is also a vital measure, but it usually makes the purification system too complicated to be employed in a living place. Moreover, plasma can be an economical and effective way to improve the charge of submicron aerosols and promote the collision process simultaneously.

(2) As for the deactivation of microbial aerosols, traditional electrostatic precipitation was usually thought to be preliminary inactivation with ions and ozone. The mechanism is also general and vague. At the same time, the effect of reactive species generated by plasma on the inactivation of microorganisms is more distinct and well-studied. Among the numerous kinds of RONS, short-living species like $^1O_2$ are more crucial than long-living species. Adjusting and controlling environmental factors is highly effective in making better use of the short-living species.

(3) The modeling research of collection by the electrostatic device is nearly complete, but it needs to be further developed for the numerical simulation model of electrostatic inactivation. Currently, more and more attention has been paid to predicting the distribution of survival microbial aerosol by employing the disinfection coefficient.

(4) The multifarious innovative research progress in electrostatic air purifying equipment is of high reference value for designing and integrating an application-level air purifying system toward individual demand. The core of these technologies is to optimize the electric field strength of the discharge to keep the balance between the collection efficiency and byproducts like ozone. Although the research about catalytic material for the removal and conversion of byproducts has been very mature, the integration of the electrostatic and catalytic systems is still not perfect.

Moreover, there are few outlooks on future development in research about electrostatic air purification based on the recent progress.

(1) In-depth analysis of the inactivation mechanism of microorganisms under multifield coupling conditions is the key to the solution to the public health crisis in the epidemic era. A single approach is no longer sufficient for eliminating air pollution composed of various pathogenic species in public. The *in situ* research about the inactivation process of airborne microorganisms is not as adequate as that in water treatment. In the future, it needs to explore further how to realize the accurate in situ observation of the collection and inactivation of airborne organisms in the electrostatic field.

(2) One of the most crucial research hotspots in the future is the optimization of contradiction and coordination between harmful byproduct generation and purification

https://doi.org/10.1021/envhealth.4c00100
Environ. Health 2024, 2, 596−617

efficiency. Both long-lived RONS (H_2O_2, O_3, etc.) and short-lived RONS ($ONOO^-$ and $^1O_2$, etc.) are the main reaction species generated by the electric field, which may have beneficial and controversial effects simultaneously in the application. Combining the parameter regulation of the electrostatic device and pollutant after-treatment could be a helpful pathway for the question.

(3) Based on existing numerical models for predicting microbial inactivation by electrostatic device, it is essential to establish the simulation model of disinfection by ozone generated from corona discharge. It is beneficial to construct comprehensive simulation tools for research and engineering.

(4) Developing energy-saving and efficient microbial aerosol inactivation technology is fundamental for promoting electrostatic disinfection methods. Most plasma generators are based on AC power, which restrained the application of high-efficiency technology. More efforts should be transferred to the field of DC power-driving plasma generators in the future. And more renewable energy would be involved, such as visible light, etc. Based on a few special reports on solar-driven air filters, there should be a more efficient and broad-spectrum novel system in the future.

■ AUTHOR INFORMATION

Corresponding Authors

Wenfeng Shangguan − *Research Center for Combustion and Environmental Technology, School of Mechanical Engineering, Shanghai Jiao Tong University, Shanghai 200240, PR China*; orcid.org/0000-0001-9229-2845; Email: shangguan@sjtu.edu.cn

Yong Zhu − *School of Mechanical and Power Engineering, East China University of Science and Technology, Shanghai 200237, PR China*; Email: zyong@ecust.edu.cn

Authors

Shanlong Tao − *Research Center for Combustion and Environmental Technology, School of Mechanical Engineering, Shanghai Jiao Tong University, Shanghai 200240, PR China*

Mingxia Chen − *Research Center for Combustion and Environmental Technology, School of Mechanical Engineering, Shanghai Jiao Tong University, Shanghai 200240, PR China*

Complete contact information is available at: https://pubs.acs.org/10.1021/envhealth.4c00100

Notes

The authors declare no competing financial interest.

■ ACKNOWLEDGMENTS

This work was supported by the National Key Research & Development Plan (2017YFC0211804) and the National Natural Science Foundation of China (21577088, 22176123).

■ REFERENCES

(1) Wang, Y.; Han, Y.; Zhu, T.; Li, W.; Zhang, H. A prospective study (SCOPE) comparing the cardiometabolic and respiratory effects of air pollution exposure on healthy and pre-diabetic individuals. *Sci. China Life Sci.* **2018**, *61* (1), 46−56.

(2) Wang, L.; Zheng, X.; Stevanovic, S.; Xiang, Z.; Liu, J.; Shi, H.; Liu, J.; Yu, M.; Zhu, C. Characterizing pollutant emissions from mosquito repellents incenses and implications in risk assessment of human health. *Chemosphere* **2018**, *191*, 962−970.

(3) Mukherjee, S.; Boral, S.; Siddiqi, H.; Mishra, A.; Meikap, B. C. Present cum future of SARS-CoV-2 virus and its associated control of virus-laden air pollutants leading to potential environmental threat - A global review. *J. Environ. Chem. Eng.* **2021**, *9* (2), No. 104973.

(4) Brankston, G.; Gitterman, L.; Hirji, Z.; Lemieux, C.; Gardam, M. Transmission of influenza A in human beings. *Lancet Infect. Dis.* **2007**, *7* (4), 257−265.

(5) Mohan, S. V.; Hemalatha, M.; Kopperi, H.; Ranjith, I.; Kumar, A. K. SARS-CoV-2 in environmental perspective: Occurrence, persistence, surveillance, inactivation and challenges. *Chem. Eng. J.* **2021**, *405*, No. 126893.

(6) Azimi, P.; Stephens, B. HVAC filtration for controlling infectious airborne disease transmission in indoor environments: Predicting risk reductions and operational costs. *Build. Environ.* **2013**, *70*, 150−160.

(7) Wenke, C.; Pospiech, J.; Reutter, T.; Truyen, U.; Speck, S. Efficiency of different air filter types for pig facilities at laboratory scale. *PLoS One* **2017**, *12* (10), No. e0186558.

(8) Berry, G.; Parsons, A.; Morgan, M.; Rickert, J.; Cho, H. A review of methods to reduce the probability of the airborne spread of COVID-19 in ventilation systems and enclosed spaces. *Environ. Res.* **2022**, *203*, No. 111765.

(9) Banik, S.; Bandyopadhyay, S.; Ganguly, S. Bioeffects of microwave−−a brief review. *Bioresour. Technol.* **2003**, *87* (2), 155−159. Bozkurt-Cekmer, H.; Davidson, P. Microwaves for microbial inactivation—efficiency and inactivation kinetics. In *The microwave processing of foods*; Elsevier, 2017; pp 220−251.

(10) Bintsis, T.; Litopoulou-Tzanetaki, E.; Robinson, R. K Existing and potential applications of ultraviolet light in the food industry − a critical review. *J. Sci. Food Agric.* **2000**, *80* (6), 637−645.

(11) Ma, X.; Lv, Y.; Xu, J.; Liu, Y.; Zhang, R.; Zhu, Y. A Strategy of Enhancing the Photoactivity of g-C3N4 via Doping of Nonmetal Elements: A First-Principles Study. *J. Phys. Chem. C* **2012**, *116* (44), 23485−23493.

(12) Pelaez, M.; Nolan, N. T.; Pillai, S. C.; Seery, M. K.; Falaras, P.; Kontos, A. G.; Dunlop, P. S.M.; Hamilton, J. W.J.; Byrne, J.A.; O'Shea, K.; Entezari, M. H.; Dionysiou, D. D. A review on the visible light active titanium dioxide photocatalysts for environmental applications. *Appl. Catal., B* **2012**, *125*, 331−349.

(13) Ahmadi, Y.; Bhardwaj, N.; Kim, K. H.; Kumar, S. Recent advances in photocatalytic removal of airborne pathogens in air. *Sci. Total Environ.* **2021**, *794*, No. 148477.

(14) Ma, Z.; Dwivedi, A. K.; Clack, H. L. Effects of chemically-reductive trace gas contaminants on non-thermal plasma inactivation of an airborne virus. *Sci. Total Environ.* **2024**, *939*, No. 173447.

(15) De Gabory, L.; Alharbi, A.; Kérimian, M.; Lafon, M.-E. The influenza virus, SARS-CoV-2, and the airways: Clarification for the otorhinolaryngologist. *Eur. Ann. Otorhinolaryngol. Head Neck Dis.* **2020**, *137* (4), 291−296.

(16) Anand, S.; Mayya, Y. Size distribution of virus laden droplets from expiratory ejecta of infected subjects. *Sci. Rep.* **2020**, *10* (1), 1−9.

(17) Górny, R. L.; Fraczek, K.; Ropek, D. R. Size distribution of microbial aerosols in overground and subterranean treatment chambers at health resorts. *J. Environ. Health Sci. Eng.* **2020**, *18* (2), 1437−1450.

(18) Gong, J.; Qi, J.; E, B.; Yin, Y.; Gao, D. Concentration, viability and size distribution of bacteria in atmospheric bioaerosols under different types of pollution. *Environ. Pollut.* **2020**, *257*, No. 113485.

(19) Jaworek, A.; Marchewicz, A.; Sobczyk, A. T.; Krupa, A.; Czech, T. Two-stage electrostatic precipitators for the reduction of PM2.5 particle emission. *Prog. Energy Combust. Sci.* **2018**, *67*, 206−233.

(20) de Aquino Lima, F.; Guerra, V. G. Collection of nanoparticles by electrostatic precipitation operating over a wide range of electric fields. *Sep. Sci. Technol.* **2024**, *59* (5), 848−865.

(21) Chen, L.; Gonze, E.; Ondarts, M.; Outin, J.; Gonthier, Y. Electrostatic precipitator for fine and ultrafine particle removal from indoor air environments. *Sep. Purif. Technol.* **2020**, *247*, No. 116964.
(22) Wang, P.; Liu, J.; Wang, C.; Zhang, Z.; Li, J. A holistic performance assessment of duct-type electrostatic precipitators. *J. Clean. Prod.* **2022**, *357*, No. 131997.
(23) Aboubakr, H. A.; Mor, S. K.; Higgins, L.; Armien, A.; Youssef, M. M.; Bruggeman, P. J.; Goyal, S. M. Cold argon-oxygen plasma species oxidize and disintegrate capsid protein of feline calicivirus. *PLoS One* **2018**, *13* (3), No. e0194618.
(24) Guo, H.; Chen, J.; Wang, L.; Wang, A. C.; Li, Y.; An, C.; He, J.-H.; Hu, C.; Hsiao, V. K. S.; Wang, Z. L. A highly efficient triboelectric negative air ion generator. *Nat. Sustain.* **2021**, *4* (2), 147−153.
(25) Xiao, S.; Wei, T.; Petersen, J. D.; Zhou, J.; Lu, X. Biological effects of negative air ions on human health and integrated multiomics to identify biomarkers: a literature review. *Environ. Sci. Pollut. Res.* **2023**, *30* (27), 69824−69836.
(26) Murray, B. K.; Ohmine, S.; Tomer, D. P.; Jensen, K. J.; Johnson, F. B.; Kirsi, J. J.; Robison, R. A.; O'Neill, K. L. Virion disruption by ozone-mediated reactive oxygen species. *J. Virol. Methods* **2008**, *153* (1), 74−77.
(27) Mo, J.; Tian, E.; Pan, J. New electrostatic precipitator with dielectric coatings to efficiently and safely remove sub-micro particles in the building environment. *Sustain. Cities Soc.* **2020**, *55*, No. 102063.
(28) Gao, M.; Zhu, Y.; Yao, X.; Shi, J.; Shangguan, W. Dust removal performance of two-stage electrostatic precipitators and its influencing factors. *Powder Technol.* **2019**, *348*, 13−23.
(29) Li, L.; Gopalakrishnan, R. An experimentally validated model of diffusion charging of arbitrary shaped aerosol particles. *J. Aerosol Sci.* **2021**, *151*, No. 105678.
(30) Zhu, Y.; Tao, S.; Chen, C.; Liu, J.; Chen, M.; Shangguan, W. A novel approach for evaluating the effect of external electric field on charged particles based on the Lagrangian particle tracking method. *Powder Technol.* **2021**, *394*, 92−102.
(31) Zukeran, A.; Ikeda, Y.; Ehara, Y.; Matsuyama, M.; Ito, T.; Takahashi, T.; Kawakami, H.; Takamatsu, T. Two-stage-type electrostatic precipitator re-entrainment phenomena under diesel flue gases. *IEEE Trans. Ind. Appl.* **1999**, *35* (2), 346−351.
(32) Xing Jin, S. L.; Yang, M.M; Zhou, J.K.; Yao, Q. Investigation on the Packing of Fine Particles in Presemce of High-Voltage Electric Field. *J. Eng. Thermophys.* **2012**, *33* (3), 533−536.
(33) Zhu, Y.; Zhang, Y.; Yang, X.; Tao, S.; Chen, M.; Shangguan, W. Operando investigation of particle re-entrainment mechanism in electrostatic capture process on the lab-on-a-chip. *J. Environ. Sci.* **2024**, *136*, 337−347.
(34) Zhu, Y.; Tao, S.; Yang, X.; Zhang, Y.; Chen, M.; Shao, Z.; Shangguan, W. Operando investigation of deposition characteristics of submicron particles in electric-flow coupled fields combined with object detection. *Fuel* **2024**, *358*, No. 130348.
(35) Tao, S.; Zhu, Y.; Chen, M.; Jiang, Z.; Shangguan, W. Mechanism of submicron particle dendrite agglomeration growth and fracture in flow-electric coupling field. *Chem. Eng. Sci.* **2024**, *296*, No. 120213.
(36) Li, Y.; Fan, Z.; Shi, J.; Liu, Z.; Zhou, J.; Shangguan, W. Removal of Volatile Organic Compounds (VOCs) at Room Temperature Using Dielectric Barrier Discharge and Plasma-Catalysis. *Plasma Chem. Plasma Process.* **2014**, *34* (4), 801−810.
(37) Li, Y.; Fan, Z.; Shi, J.; Liu, Z.; Zhou, J.; Shangguan, W. Modified manganese oxide octahedral molecular sieves M′-OMS-2 (M′ = Co,Ce,Cu) as catalysts in post plasma-catalysis for acetaldehyde degradation. *Catal. Today* **2015**, *256*, 178−185.
(38) Khezami, L.; Nguyen-Tri, P.; Saoud, W. A.; Bouzaza, A.; El Jery, A.; Duc Nguyen, D.; Gupta, V. K.; Assadi, A. A. Recent progress in air treatment with combined photocatalytic/plasma processes: A review. *J. Environ. Manage.* **2021**, *299*, No. 113588.
(39) Jõgi, I.; Erme, K.; Levoll, E.; Raud, J.; Stamate, E. Plasma and catalyst for the oxidation of NOx. *Plasma Sources Sci. Technol.* **2018**, *27* (3), No. 035001.
(40) Song, C. L.; Bin, F.; Tao, Z. M.; Li, F. C.; Huang, Q. F. Simultaneous removals of NOx, HC and PM from diesel exhaust emissions by dielectric barrier discharges. *J. Hazard. Mater.* **2009**, *166* (1), 523−530.
(41) Hernandez-Diaz, D.; Martos-Ferreira, D.; Hernandez-Abad, V.; Villar-Ribera, R.; Tarres, Q.; Rojas-Sola, J. I. Indoor PM2.5 removal efficiency of two different non-thermal plasma systems. *J. Environ. Manage.* **2021**, *278*, No. 111515.
(42) Moisan, M; Barbeau, J; Moreau, S; Pelletier, J; Tabrizian, M; Yahia, L Low-temperature sterilization using gas plasmas: a review of the experiments and an analysis of the inactivation mechanisms. *Int. J. Pharm.* **2001**, *226* (1−2), 1−21.
(43) Xu, H.; Liu, C.; Huang, Q. Enhance the inactivation of fungi by the sequential use of cold atmospheric plasma and plasma-activated water: Synergistic effect and mechanism study. *Chem. Eng. J.* **2023**, *452*, No. 139596.
(44) Aranda-Rivera, A. K.; Cruz-Gregorio, A.; Arancibia-Hernández, Y. L.; Hernández-Cruz, E. Y.; Pedraza-Chaverri, J. RONS and oxidative stress: An overview of basic concepts. *Oxygen* **2022**, *2* (4), 437−478.
(45) Aboubakr, H. A.; Gangal, U.; Youssef, M. M.; Goyal, S. M.; Bruggeman, P. J. Inactivation of virus in solution by cold atmospheric pressure plasma: identification of chemical inactivation pathways. *J. Phys., D* **2016**, *49* (20), No. 204001.
(46) Filipic, A.; Gutierrez-Aguirre, I.; Primc, G.; Mozetic, M.; Dobnik, D. Cold Plasma, a New Hope in the Field of Virus Inactivation. *Trends Biotechnol.* **2020**, *38* (11), 1278−1291.
(47) Lai, A.; Cheung, A.; Wong, M.; Li, W. Evaluation of cold plasma inactivation efficacy against different airborne bacteria in ventilation duct flow. *Build. Environ.* **2016**, *98*, 39−46.
(48) Xia, T.; Yang, M.; Marabella, I.; Lee, E. M.; Olson, B.; Zarling, D.; Torremorell, M.; Clack, H. L. Inactivation of airborne porcine reproductive and respiratory syndrome virus (PRRSv) by a packed bed dielectric barrier discharge non-thermal plasma. *J. Hazard. Mater.* **2020**, *393*, No. 122266.
(49) Xiong, W.; Lin, Z.; Zhang, W.; Chen, T.; Zhao, C. Experimental and simulation studies on dust loading performance of a novel electrostatic precipitator with dielectric barrier electrodes. *Build. Environ.* **2018**, *144*, 119−128.
(50) Shi, X.; Liu, S.; Jiang, R.; Chen, J.; Jin, S.; Mei, D.; Zhou, R.; Fang, Z.; Cullen, P. J. Development and characterization of touchable air plasma jet device for inactivation of oral bacteria. *Results Phys.* **2022**, *36*, No. 105405.
(51) Berardinelli, A.; Hamrouni, A.; Dirè, S.; Ceccato, R.; Camera-Roda, G.; Ragni, L.; Palmisano, L.; Parrino, F. Features and application of coupled cold plasma and photocatalysis processes for decontamination of water. *Chemosphere* **2021**, *262*, No. 128336.
(52) Gao, Y.; Tian, E.; Mo, J. Electrically Responsive Coarse Filters Endowed by High-Dielectric-Constant Surface Coatings toward Efficient Removal of Ultrafine Particles and Ozone. *ACS ES&T Engg.* **2021**, *1* (10), 1449−1459.
(53) Zhu, Y.; Gao, M.; Chen, M.; Shi, J.; Shangguan, W. Numerical simulation of capture process of fine particles in electrostatic precipitators under consideration of electrohydrodynamics flow. *Powder Technol.* **2019**, *354*, 653−675.
(54) Zhu, Y.; Tao, S.; Chen, C.; Liu, J.; Chen, M.; Shangguan, W. Highly effective removal of PM2.5 from combustion products: An application of integrated two-stage electrostatic precipitator. *Chem. Eng. J.* **2021**, *424*, No. 130569.
(55) Byeon, J. H.; Hwang, J.; Hong Park, J.; Young Yoon, K.; Ju Ko, B.; Hoon Kang, S.; Ho Ji, J. Collection of submicron particles by an electrostatic precipitator using a dielectric barrier discharge. *J. Aerosol Sci.* **2006**, *37* (11), 1618−1628.
(56) Zhu, Y.; Chen, C.; Shi, J.; Chen, M.; Shangguan, W. Experimental investigation of the effect of collection length in a two-stage electrostatic precipitator for removal of PM2.5. *Chem. Eng. J.* **2021**, *421*, No. 127797.
(57) Zhu, Y.; Chen, C.; Shi, J.; Shangguan, W. Enhancement of air purification by unique W-plate structure in two-stage electrostatic

precipitator: A novel design for efficient capture of fine particles. *Adv. Powder Technol.* **2020**, *31* (4), 1643−1658.

(58) Tian, E.; Yu, Q.; Gao, Y.; Wang, H.; Wang, C.; Zhang, Y.; Li, B.; Zhu, M.; Mo, J.; Xu, G.; Li, J. Ultralow Resistance Two-Stage Electrostatically Assisted Air Filtration by Polydopamine Coated PET Coarse Filter. *Small* **2021**, *17* (33), No. 2102051.

(59) Yao, M.; Mainelis, G.; An, H. R. Inactivation of microorganisms using electrostatic fields. *Environ. Sci. Technol.* **2005**, *39* (9), 3338−3344.

(60) Podliński, J.; Niewulis, A.; Mizeraczyk, J. Electrohydrodynamic flow and particle collection efficiency of a spike-plate type electrostatic precipitator. *J. Electrost.* **2009**, *67* (2−3), 99−104.

(61) Li, Z.; Liu, Y.; Xing, Y.; Tran, T. M.; Le, T. C.; Tsai, C. J. Novel Wire-on-Plate Electrostatic Precipitator (WOP-EP) for Controlling Fine Particle and Nanoparticle Pollution. *Environ. Sci. Technol.* **2015**, *49* (14), 8683−8690.

(62) Zhu, Y.; Chen, C.; Chen, M.; Shi, J.; Shangguan, W. Numerical simulation of electrostatic field and its influence on submicron particle charging in small-sized charger for consideration of voltage polarity. *Powder Technol.* **2021**, *380*, 183−198.

(63) Tao, S.; Zhu, Y.; Chen, C.; Liu, J.; Chen, M.; Shangguan, W. Removal of air pollutant by a spike-tubular electrostatic device: Multi-stage direct current corona discharge enhanced electrostatic precipitation and oxidation ability. *Process Saf. Environ. Prot.* **2022**, *165*, 347−356.

(64) Liu, X.; Wang, Y.; Gao, Y.; Liu, C.; Mo, J. Design and performance of a novel miniaturized electrostatic sampler for efficient airborne particulate matter sampling. *Build. Simul.* **2023**, *16* (8), 1439−1450.

(65) Carotenuto, C.; Di Natale, F.; Lancia, A. Wet electrostatic scrubbers for the abatement of submicronic particulate. *Chem. Eng. J.* **2010**, *165* (1), 35−45.

(66) Krueger, A. P.; Reed, E. J. Biological Impact of Small Air Ions: Despite a history of contention, there is evidence that small air ions can affect life processes. *Science* **1976**, *193* (4259), 1209−1213.

(67) Phadke, K. S.; Madival, D. G.; Venkataraman, J.; Kundu, D.; Ramanujan, K.; Holla, N.; Arakeri, J.; Tomar, G.; Datta, S.; Ghatak, A. Novel non intrusive continuous use ZeBox technology to trap and kill airborne microbes. *Sci. Rep.* **2021**, *11* (1), 1−9.

(68) Huo, Z. Y.; Xie, X.; Yu, T.; Lu, Y.; Feng, C.; Hu, H. Y. Nanowire-Modified Three-Dimensional Electrode Enabling Low-Voltage Electroporation for Water Disinfection. *Environ. Sci. Technol.* **2016**, *50* (14), 7641−7649.

(69) Kettleson, E. M.; Ramaswami, B.; Hogan, C. J., Jr; Lee, M.-H.; Statyukha, G. A.; Biswas, P.; Angenent, L. T. Airborne virus capture and inactivation by an electrostatic particle collector. *Environ. Sci. Technol.* **2009**, *43* (15), 5940−5946.

(70) Chang, Q.; Zheng, C.; Gao, X.; Chiang, P.; Fang, M.; Luo, Z.; Cen, K. Systematic Approach to Optimization of Submicron Particle Agglomeration Using Ionic-Wind-Assisted Pre-Charger. *Aerosol Air Qual. Res.* **2015**, *15* (7), 2709−2719.

(71) Kim, H.-J.; Han, B.; Kim, Y.-J.; Yoa, S.-J. Characteristics of an electrostatic precipitator for submicron particles using non-metallic electrodes and collection plates. *J. Aerosol Sci.* **2010**, *41* (11), 987−997.

(72) Kim, H. J.; Han, B.; Kim, Y. J.; Oda, T.; Won, H. Submicrometer particle removal indoors by a novel electrostatic precipitator with high clean air delivery rate, low ozone emissions, and carbon fiber ionizer. *Indoor Air* **2013**, *23* (5), 369−378.

(73) Xia, F.; Chen, Z.; Gao, Y.; Tian, E.; Mo, J. Simultaneous Capture and Inactivation of Airborne Bacteria by a Dual-Zone Electrostatically Actuated Filter. *ACS ES&T Engg.* **2024**, *4* (4), 987−994.

(74) Sim, K. M.; Park, H. S.; Bae, G. N.; Jung, J. H. Antimicrobial nanoparticle-coated electrostatic air filter with high filtration efficiency and low pressure drop. *Sci. Total Environ.* **2015**, *533*, 266−274.

(75) Zhang, P.; Zhang, S.; Wan, D.; Zhang, P.; Zhang, Z.; Shao, G. Multilevel polarization-fields enhanced capture and photocatalytic conversion of particulate matter over flexible schottky-junction nanofiber membranes. *J. Hazard. Mater.* **2020**, *395*, No. 122639.

(76) Narayan, R.; Kundu, D.; Ghatak, A.; Tripathi, S.; Datta, S. Efficient Elimination of Airborne Pathogens: A Study on aerosolized Mycobacterium tuberculosis and SARS-CoV-2 using ZeBox Technology. *J. Hosp. Infec.* **2022**, *129*, 17−21.

(77) Sale, A.; Hamilton, W. Effects of high electric fields on microorganisms: I. Killing of bacteria and yeasts. *Biochim. Biophys. Acta* **1967**, *148* (3), 781−788.

(78) Huo, Z.-Y.; Zhou, J.-F.; Wu, Y.; Wu, Y.-H.; Liu, H.; Liu, N.; Hu, H.-Y.; Xie, X. A Cu_3P nanowire enabling high-efficiency, reliable, and energy-efficient low-voltage electroporation-inactivation of pathogens in water. *J. Mater. Chem. A* **2018**, *6* (39), 18813−18820.

(79) Huo, Z. Y.; Kim, Y. J.; Suh, I. Y.; Lee, D. M.; Lee, J. H.; Du, Y.; Wang, S.; Yoon, H. J.; Kim, S. W. Triboelectrification induced self-powered microbial disinfection using nanowire-enhanced localized electric field. *Nat. Commun.* **2021**, *12* (1), 3693.

(80) Zhou, J.; Wang, T.; Yu, C.; Xie, X. Locally enhanced electric field treatment (LEEFT) for water disinfection. *Front. Environ. Sci. Eng.* **2020**, *14* (5), 1−12.

(81) Wang, T.; Brown, D. K.; Xie, X. Operando Investigation of Locally Enhanced Electric Field Treatment (LEEFT) Harnessing Lightning-Rod Effect for Rapid Bacteria Inactivation. *Nano Lett.* **2022**, *22* (2), 860−867.

(82) He, W.; Guo, Y.; Zhao, Y.-B.; Jiang, F.; Schmitt, J.; Yue, Y.; Liu, J.; Cao, J.; Wang, J. Self-supporting smart air filters based on PZT/PVDF electrospun nanofiber composite membrane. *Chem. Eng. J.* **2021**, *423*, No. 130247.

(83) Pillet, F.; Formosa-Dague, C.; Baaziz, H.; Dague, E.; Rols, M.-P. Cell wall as a target for bacteria inactivation by pulsed electric fields. *Sci. Rep.* **2016**, *6* (1), 19778.

(84) Kellogg, E. W.; Yost, M. G.; Barthakur, N.; Kreuger, A. P. Kreuger Superoxide involvement in the bactericidal effects of negative air ions on Staphylococcus albus. *Nature* **1979**, *281*, 400−401.

(85) Badhe, R. V.; Nipate, S. S. The use of negative oxygen ion clusters [O2(−)(H2O)n] and bicarbonate ions [HCO3(−)] as the supportive treatment of COVID-19 infections: A possibility. *Med. Hypotheses* **2021**, *154*, No. 110658.

(86) Mendis, D.A.; Rosenberg, M.; Azam, F. A note on the possible electrostatic disruption of bacteria. *IEEE Transactions on Plasma Science* **2000**, *28* (4), 1304−1306. Kim, Y. S.; Yoon, K. Y.; Park, J. H.; Hwang, J. Application of air ions for bacterial de-colonization in air filters contaminated by aerosolized bacteria. *Sci. Total Environ.* **2011**, *409* (4), 748−755.

(87) Zhao, X.; Li, Y.; Hua, T.; Jiang, P.; Yin, X.; Yu, J.; Ding, B. Low-Resistance Dual-Purpose Air Filter Releasing Negative Ions and Effectively Capturing PM2.5. *ACS Appl. Mater. Interfaces* **2017**, *9* (13), 12054−12063.

(88) Park, J. H.; Yoon, K. Y.; Noh, K. C.; Byeon, J. H.; Hwang, J. Removal of PM2.5 entering through the ventilation duct in an automobile using a carbon fiber ionizer-assisted cabin air filter. *J. Aerosol Sci.* **2010**, *41* (10), 935−943.

(89) Fan, L.; Song, J.; Hildebrand, P.D.; Forney, C.F. Hildebrand and C.F. Forney. Interaction of ozone and negative air ions to control micro-organisms. *J. Appl. Microbiol.* **2002**, *93*, 144−148.

(90) Laroussi, M.; Leipold, F. Evaluation of the roles of reactive species, heat, and UV radiation in the inactivation of bacterial cells by air plasmas at atmospheric pressure. *Int. J. Mass Spectrom.* **2004**, *233* (1−3), 81−86.

(91) Hensel, K.; Kucerova, K.; Tarabova, B.; Janda, M.; Machala, Z.; Sano, K.; Mihai, C. T.; Ciorpac, M.; Gorgan, L. D.; Jijie, R.; et al. Effects of air transient spark discharge and helium plasma jet on water, bacteria, cells, and biomolecules. *Biointerphases* **2015**, *10* (2), No. 029515.

(92) Lee, G. J.; Sim, G. B.; Choi, E. H.; Kwon, Y.-W.; Kim, J. Y.; Jang, S.; Kim, S. H. Optical and structural properties of plasma-treatedCordyceps bassianaspores as studied by circular dichroism, absorption, and fluorescence spectroscopy. *J. Appl. Phys.* **2015**, *117* (2), 4905194 DOI: 10.1063/1.4905194.

(93) Wende, K.; Williams, P.; Dalluge, J.; Gaens, W. V.; Aboubakr, H.; Bischof, J.; von Woedtke, T.; Goyal, S. M.; Weltmann, K. D.; Bogaerts, A. Identification of the biologically active liquid chemistry induced by a nonthermal atmospheric pressure plasma jet. *Biointerphases* **2015**, *10* (2), 029518.
(94) Kovačević, V. V.; Dojčinović, B. P.; Jović, M.; Roglić, G. M.; Obradović, B. M.; Kuraica, M. M. Measurement of reactive species generated by dielectric barrier discharge in direct contact with water in different atmospheres. *J. Phys., D* **2017**, *50* (15), No. 155205.
(95) Piri, A.; Kim, H. R.; Hwang, J. Prevention of damage caused by corona discharge-generated reactive oxygen species under electrostatic aerosol-to-hydrosol sampling. *J. Hazard. Mater.* **2020**, *384*, No. 121477.
(96) Hamanaka, R. B.; Chandel, N. S. Mitochondrial reactive oxygen species regulate hypoxic signaling. *Curr. Opin. Cell Biol.* **2009**, *21* (6), 894−899.
(97) Christensen, P. A.; Yonar, T.; Zakaria, K. The Electrochemical Generation of Ozone: A Review. *Ozone Sci. Eng.* **2013**, *35* (3), 149−167.
(98) Cattel, F.; Giordano, S.; Bertiond, C.; Lupia, T.; Corcione, S.; Scaldaferri, M.; Angelone, L.; De Rosa, F. G. Ozone therapy in COVID-19: A narrative review. *Virus Res.* **2021**, *291*, No. 198207.
(99) Chirumbolo, S.; Valdenassi, L.; Simonetti, V.; Bertossi, D.; Ricevuti, G.; Franzini, M.; Pandolfi, S. Insights on the mechanisms of action of ozone in the medical therapy against COVID-19. *Int. Immunopharmacol.* **2021**, *96*, No. 107777.
(100) Izadi, M.; Cegolon, L.; Javanbakht, M.; Sarafzadeh, A.; Abolghasemi, H.; Alishiri, G.; Zhao, S.; Einollahi, B.; Kashaki, M.; Jonaidi-Jafari, N.; et al. Ozone therapy for the treatment of COVID-19 pneumonia: A scoping review. *Int. Immunopharmacol.* **2021**, *92*, No. 107307.
(101) Tamaddon Jahromi, H.; Rolland, S.; Jones, J.; Coccarelli, A.; Sazonov, I.; Kershaw, C.; Tizaoui, C.; Holliman, P.; Worsley, D.; Thomas, H.; Nithiarasu, P. Modelling ozone disinfection process for creating COVID-19 secure spaces. *Int. J. Numer. Method. Heat Fluid Flow* **2022**, *32* (1), 353−363.
(102) Tizaoui, C. Ozone: A Potential Oxidant for COVID-19 Virus (SARS-CoV-2). *Ozone Sci. Eng.* **2020**, *42* (5), 378−385.
(103) Alimohammadi, M.; Naderi, M. Effectiveness of Ozone Gas on Airborne Virus Inactivation in Enclosed Spaces: A Review Study. *Ozone Sci. Eng.* **2021**, *43* (1), 21−31.
(104) Bayarri, B.; Cruz-Alcalde, A.; Lopez-Vinent, N.; Mico, M. M.; Sans, C. Can ozone inactivate SARS-CoV-2? A review of mechanisms and performance on viruses. *J. Hazard. Mater.* **2021**, *415*, No. 125658.
(105) Hudson, J. B.; Sharma, M.; Vimalanathan, S. Development of a practical method for using ozone gas as a virus decontaminating agent. *Ozone Sci. Eng.* **2009**, *31* (3), 216−223.
(106) Tseng, C.-C.; Li, C.-S. Ozone for Inactivation of Aerosolized Bacteriophages. *Aerosol Sci. Technol.* **2006**, *40* (9), 683−689.
(107) Xia, T.; Kleinheksel, A.; Lee, E. M.; Qiao, Z.; Wigginton, K. R.; Clack, H. L. Inactivation of airborne viruses using a packed bed non-thermal plasma reactor. *J. Phys., D* **2019**, *52* (25), No. 255201.
(108) Guo, L.; Xu, R.; Gou, L.; Liu, Z.; Zhao, Y.; Liu, D.; Zhang, L.; Chen, H.; Kong, M. G. Mechanism of Virus Inactivation by Cold Atmospheric-Pressure Plasma and Plasma-Activated Water. *Appl. Environ. Microbiol.* **2018**, *84* (17), 1−10.
(109) Yamashiro, R.; Misawa, T.; Sakudo, A. Key role of singlet oxygen and peroxynitrite in viral RNA damage during virucidal effect of plasma torch on feline calicivirus. *Sci. Rep.* **2018**, *8*, 17947.
(110) Hotze, E. M.; Badireddy, A. R.; Chellam, S.; Wiesner, M. R. Mechanisms of bacteriophage inactivation via singlet oxygen generation in UV illuminated fullerol suspensions. *Environ. Sci. Technol.* **2009**, *43* (17), 6639−6645.
(111) Nayak, G.; Aboubakr, H. A.; Goyal, S. M.; Bruggeman, P. J. Reactive species responsible for the inactivation of feline calicivirus by a two-dimensional array of integrated coaxial microhollow dielectric barrier discharges in air. *Plasma Process. Polym.* **2018**, *15* (1), No. 1700119.
(112) Zimmermann, J. L.; Dumler, K.; Shimizu, T.; Morfill, G. E.; Wolf, A.; Boxhammer, V.; Schlegel, J.; Gansbacher, B.; Anton, M. Effects of cold atmospheric plasmas on adenoviruses in solution. *J. Phys., D* **2011**, *44* (50), No. 505201.
(113) van Gils, C. A. J.; Hofmann, S.; Boekema, B. K. H. L.; Brandenburg, R.; Bruggeman, P. J. Mechanisms of bacterial inactivation in the liquid phase induced by a remote RF cold atmospheric pressure plasma jet. *J. Phys., D* **2013**, *46* (17), No. 175203.
(114) Zhu, L.; Gunn, C.; Beckman, J. S. Bactericidal activity of peroxynitrite. *Arch. Biochem. Biophys.* **1992**, *298* (2), 452−457.
(115) Gao, H.; Wang, G.; Chen, B.; Zhang, Y.; Liu, D.; Lu, X.; He, G.; Ostrikov, K. Atmospheric-pressure non-equilibrium plasmas for effective abatement of pathogenic biological aerosols. *Plasma Sources Sci. Technol.* **2021**, *30* (5), No. 053001.
(116) Lu, X.; Naidis, G. V.; Laroussi, M.; Reuter, S.; Graves, D. B.; Ostrikov, K. Reactive species in non-equilibrium atmospheric-pressure plasmas: Generation, transport, and biological effects. *Phys. Rep.* **2016**, *630*, 1−84.
(117) Cui, J.; Yeasmin, R.; Shao, Y.; Zhang, H.; Zhang, H.; Zhu, J. Fabrication of Ag+, Cu2+, and Zn2+ ternary ion-exchanged zeolite as an antimicrobial agent in powder coating. *Ind. Eng. Chem. Res.* **2020**, *59* (2), 751−762.
(118) Zhang, L.; Chen, J.; Yu, W.; Zhao, Q.; Liu, J. Antimicrobial nanocomposites prepared from montmorillonite/Ag+/quaternary ammonium nitrate. *J. Nanomater.* **2018**, *2018* (1), No. 6190251.
(119) Je, J.-Y.; Kim, S.-K. Chitosan derivatives killed bacteria by disrupting the outer and inner membrane. *J. Agric. Food Chem.* **2006**, *54* (18), 6629−6633.
(120) Raafat, D.; Von Bargen, K.; Haas, A.; Sahl, H.-G. Insights into the mode of action of chitosan as an antibacterial compound. *Appl. Environ. Microbiol.* **2008**, *74* (12), 3764−3773.
(121) Sun, Z.; Yue, Y.; He, W.; Jiang, F.; Lin, C.-H.; Pui, D. Y. H.; Liang, Y.; Wang, J. The antibacterial performance of positively charged and chitosan dipped air filter media. *Build. Environ.* **2020**, *180*, No. 107020.
(122) Cooperman, P. A new theory of precipitator efficiency. *Atmos. Environ.* **1971**, *5* (7), 541−551.
(123) Zhibin, Z.; Guoquan, Z. Investigations of the collection efficiency of an electrostatic precipitator with turbulent effects. *Aerosol Sci. Technol.* **1994**, *20* (2), 169−176.
(124) Adamiak, K. Numerical models in simulating wire-plate electrostatic precipitators: A review. *J. Electrost.* **2013**, *71* (4), 673−680.
(125) Kim, H. J.; Han, B.; Kim, Y. J.; Hwang, K. D.; Oh, W. S.; Yoo, S. Y.; Oda, T. Fine particle removal performance of a two-stage wet electrostatic precipitator using a nonmetallic pre-charger. *J. Air Waste Manag. Assoc.* **2011**, *61* (12), 1334−1343.
(126) Yoon, K. Y.; Hoon Byeon, J.; Park, J. H.; Hwang, J. Susceptibility constants of Escherichia coli and Bacillus subtilis to silver and copper nanoparticles. *Sci. Total Environ.* **2007**, *373* (2−3), 572−575.
(127) Oglesby, S.; Nichols, G. *Electrostatic Precipitation* Marcel Dekker, New York. NY. 1978.
(128) Riehle, C.; Löfer, F. Grade efficiency and eddy diffusivity models. *J. Electrost.* **1995**, *34* (4), 401−413.
(129) Chen, C.; Zhu, Y.; Chen, M.; Shangguan, W. A novel approach for investigation of collision mechanisms between fine particles in electrostatic precipitator under consideration of Brownian effect. *Chem. Eng. Res. Des.* **2021**, *168*, 96−108.
(130) Zhu, Y.; Tao, S.; Chen, C.; Liu, J.; Chen, M.; Shangguan, W. The experimental and simulation investigation of the dynamic characteristic of submicron-scale aerosol in high-voltage electric field by a visualization method. *J. Hazard.Mater.* **2021**, *416*, No. 126227.
(131) Falco, I.; Randazzo, W.; Sanchez, G.; Vilarroig, J.; Climent, J.; Chiva, S.; Chica, A.; Navarro-Laboulais, J. Experimental and CFD evaluation of ozone efficacy against coronavirus and enteric virus

contamination on public transport surfaces. *J. Environ. Chem. Eng.* **2021**, *9* (5), No. 106217.

(132) Petry, G.; Rossato, L. G.; Nespolo, J.; Kreutz, L. C.; Bertol, C. D. In vitro inactivation of herpes virus by ozone. *Ozone Sci. Eng.* **2014**, *36* (3), 249−252.

(133) Dubuis, M.-E.; Dumont-Leblond, N.; Laliberté, C.; Veillette, M.; Turgeon, N.; Jean, J.; Duchaine, C. Ozone efficacy for the control of airborne viruses: Bacteriophage and norovirus models. *PLoS One* **2020**, *15* (4), No. e0231164.

(134) Dennis, R.; Cashion, A.; Emanuel, S.; Hubbard, D. Ozone gas: scientific justification and practical guidelines for improvised disinfection using consumer-grade ozone generators and plastic storage boxes. *J. Sci. Med.* **2020**, *2* (1), 35 DOI: 10.37714/josam.v2i1.35.

(135) Tseng, C.; Li, C. Inactivation of surface viruses by gaseous ozone. *J. Environ. Health.* **2008**, *70* (10), 56−63.

(136) Vyskocil, J. M.; Turgeon, N.; Turgeon, J.-G.; Duchaine, C. Ozone treatment in a wind tunnel for the reduction of airborne viruses in swine buildings. *Aerosol Sci. Technol.* **2020**, *54* (12), 1471−1478.

(137) Brié, A.; Boudaud, N.; Mssihid, A.; Loutreul, J.; Bertrand, I.; Gantzer, C. Inactivation of murine norovirus and hepatitis A virus on fresh raspberries by gaseous ozone treatment. *Food Microbiol* **2018**, *70*, 1−6.

(138) Blanchard, E. L.; Lawrence, J. D.; Noble, J. A.; Xu, M.; Joo, T.; Ng, N. L.; Schmidt, B. E.; Santangelo, P. J.; Finn, M. Enveloped virus inactivation on personal protective equipment by exposure to ozone. *MedRxiv* **2020**, 20111435 DOI: 10.1101/2020.05.23.20111435.

(139) Huang, H.-L.; Lee, M.-G.; Tai, J.-H. Controlling indoor bioaerosols using a hybrid system of ozone and catalysts. *Aerosol Air Qual. Res.* **2012**, *12* (1), 73−82.

(140) De Mik, G.; De Groot, I. Mechanisms of inactivation of bacteriophage *φ*X174 and its DNA in aerosols by ozone and ozonized cyclohexene. *Epidemiol. Infect.* **1977**, *78* (2), 199−211.

(141) Cannon, J. L.; Kotwal, G.; Wang, Q. Inactivation of norovirus surrogates after exposure to atmospheric ozone. *Ozone Sci. Eng.* **2013**, *35* (3), 217−219.

(142) Clavo, B.; Cordoba-Lanus, E.; Rodriguez-Esparragon, F.; Cazorla-Rivero, S. E.; Garcia-Perez, O.; Pinero, J. E.; Villar, J.; Blanco, A.; Torres-Ascension, C.; Martin-Barrasa, J. L.; Gonzalez-Martin, J. M.; Serrano-Aguilar, P.; Lorenzo-Morales, J. Effects of ozone treatment on personal protective equipment contaminated with SARS-CoV-2. *Antioxidants* **2020**, *9* (12), 1222.

(143) SATO, H.; WANANABE, Y.; MIYATA, H. Virucidal effect of ozone treatment of laboratory animal viruses. *Exp. Anim.* **1990**, *39* (2), 223−229.

(144) Zhu, Y.; Chen, C.; Shi, J.; Shangguan, W. A novel simulation method for predicting ozone generation in corona discharge region. *Chem. Eng. Sci.* **2020**, *227*, No. 115910.

(145) Kim, Y. S.; Yoon, K. Y.; Park, J. H.; Hwang, J. Application of air ions for bacterial de-colonization in air filters contaminated by aerosolized bacteria. *Sci. Total Environ.* **2011**, *409* (4), 748−755.

(146) Nunayon, S. S.; Zhang, H. H.; Jin, X.; Lai, A. C. K. Experimental evaluation of positive and negative air ions disinfection efficacy under different ventilation duct conditions. *Build. Environ.* **2019**, *158*, 295−301.

(147) Kang, M.; Jang, N.-Y.; Kim, Y.-J.; Ro, H.-J.; Kim, D.; Kim, Y.; Kim, H. T.; Kwon, H. M.; Ahn, J.-H.; Choi, B.-O.; Cho, N.-H.; Kim, S.-W. Virus blocking textile for SARS-CoV-2 using human body triboelectric energy harvesting. *Cell Rep. Phys. Sci.* **2022**, *3* (4), No. 100813.

(148) Peleg, M. *Advanced quantitative microbiology for foods and biosystems: models for predicting growth and inactivation*; CRC Press, 2006.

(149) Peleg, M.; Normand, M.; Corradini, M. Generating microbial survival curves during thermal processing in real time. *J. Appl. Microbiol.* **2005**, *98* (2), 406−417.

(150) Corradini, M. G. Modeling microbial inactivation during cold atmospheric-pressure plasma (CAPP) processing. *Advances in Cold Plasma Applications for Food Safety and Preservation* **2020**, 93−108.

(151) Rossow, M.; Ludewig, M.; Braun, P. G. Effect of cold atmospheric pressure plasma treatment on inactivation of Campylobacter jejuni on chicken skin and breast fillet. *LWT* **2018**, *91*, 265−270.

(152) Liao, X.; Li, J.; Muhammad, A. I.; Suo, Y.; Chen, S.; Ye, X.; Liu, D.; Ding, T. Application of a dielectric barrier discharge atmospheric cold plasma (Dbd-Acp) for Eshcerichia coli inactivation in apple juice. *J. Food Sci.* **2018**, *83* (2), 401−408.

(153) Santos, L., Jr; Cubas, A.; Moecke, E.; Ribeiro, D.; Amante, E. Use of cold plasma to inactivate Escherichia coli and physicochemical evaluation in pumpkin puree. *J. Food Prot.* **2018**, *81* (11), 1897−1905.

(154) Prasad, P.; Mehta, D.; Bansal, V.; Sangwan, R. S. Effect of atmospheric cold plasma (ACP) with its extended storage on the inactivation of Escherichia coli inoculated on tomato. *Food Res. Int.* **2017**, *102*, 402−408.

(155) Waskow, A.; Betschart, J.; Butscher, D.; Oberbossel, G.; Klöti, D.; Büttner-Mainik, A.; Adamcik, J.; Von Rohr, P. R.; Schuppler, M. Characterization of efficiency and mechanisms of cold atmospheric pressure plasma decontamination of seeds for sprout production. *Front. Microbiol.* **2018**, *9*, 3164.

(156) Mošovská, S.; Medvecká, V.; Halászová, N.; Durina, P.; Valík, L'.; Mikulajová, A.; Zahoranová, A. Cold atmospheric pressure ambient air plasma inhibition of pathogenic bacteria on the surface of black pepper. *Food Res. Int.* **2018**, *106*, 862−869.

(157) Lee, T.; Puligundla, P.; Mok, C. Corona discharge plasma jet inactivates food-borne pathogens adsorbed onto packaging material surfaces. *Packag. Technol. Sci.* **2017**, *30* (10), 681−690.

(158) Calvo, T.; Álvarez-Ordóñez, A.; Prieto, M.; González-Raurich, M.; López, M. Influence of processing parameters and stress adaptation on the inactivation of Listeria monocytogenes by Non-Thermal Atmospheric Plasma (NTAP). *Food Res. Int.* **2016**, *89*, 631−637.

(159) Kilonzo-Nthenge, A.; Liu, S.; Yannam, S.; Patras, A. Atmospheric cold plasma inactivation of Salmonella and Escherichia coli on the surface of golden delicious apples. *Front. Nutr.* **2018**, *5*, 120.

(160) Dasan, B. G.; Yildirim, T.; Boyaci, I. H. Surface decontamination of eggshells by using non-thermal atmospheric plasma. *Int. J. Food Microbiol.* **2018**, *266*, 267−273.

(161) Kim, J. H.; Min, S. C. Moisture vaporization-combined helium dielectric barrier discharge-cold plasma treatment for microbial decontamination of onion flakes. *Food Control* **2018**, *84*, 321−329.

(162) Huang, Y.; Ye, X. P.; Doona, C. J.; Feeherry, F. E.; Radosevich, M.; Wang, S. An investigation of inactivation mechanisms of Bacillus amyloliquefaciens spores in non-thermal plasma of ambient air. *J. Sci. Food Agric.* **2019**, *99* (1), 368−378.

(163) Mendes-Oliveira, G.; Jensen, J. L.; Keener, K. M.; Campanella, O. H. Modeling the inactivation of Bacillus subtilis spores during cold plasma sterilization. *Innov. Food Sci. Emerg. Technol.* **2019**, *52*, 334−342.

(164) Butscher, D.; Zimmermann, D.; Schuppler, M.; Rudolf von Rohr, P. Plasma inactivation of bacterial endospores on wheat grains and polymeric model substrates in a dielectric barrier discharge. *Food Control* **2016**, *60*, 636−645.

(165) Zahoranová, A.; Hoppanová, L.; Šimončicová, J.; Tučeková, Z.; Medvecká, V.; Hudecová, D.; Kaliňáková, B.; Kováčik, D.; Černák, M. Effect of cold atmospheric pressure plasma on maize seeds: enhancement of seedlings growth and surface microorganisms inactivation. *Plasma Chem. Plasma Process* **2018**, *38*, 969−988.

(166) Tanino, T.; Arisaka, T.; Iguchi, Y.; Matsui, M.; Ohshima, T. Inactivation of Aspergillus sp. spores on whole black peppers by nonthermal plasma and quality evaluation of the treated peppers. *Food Control* **2019**, *97*, 94−99.

(167) Xiang, Q.; Liu, X.; Li, J.; Liu, S.; Zhang, H.; Bai, Y. Effects of dielectric barrier discharge plasma on the inactivation of Zygosacchar-

omyces rouxii and quality of apple juice. *Food Chem.* **2018**, *254*, 201−207.
(168) Wang, Y.; Wang, T.; Yuan, Y.; Fan, Y.; Guo, K.; Yue, T. Inactivation of yeast in apple juice using gas-phase surface discharge plasma treatment with a spray reactor. *Lwt* **2018**, *97*, 530−536.
(169) Yamashiro, R.; Misawa, T.; Sakudo, A. Key role of singlet oxygen and peroxynitrite in viral RNA damage during virucidal effect of plasma torch on feline calicivirus. *Sci. Rep.* **2018**, *8* (1), 17947.
(170) Lacombe, A.; Niemira, B. A.; Gurtler, J. B.; Sites, J.; Boyd, G.; Kingsley, D. H.; Li, X.; Chen, H. Nonthermal inactivation of norovirus surrogates on blueberries using atmospheric cold plasma. *Food microbiol.* **2017**, *63*, 1−5.
(171) Schmidt-Bleker, A.; Winter, J.; Iseni, S.; Dünnbier, M.; Weltmann, K. D.; Reuter, S. Reactive species output of a plasma jet with a shielding gas device—combination of FTIR absorption spectroscopy and gas phase modelling. *J. Phys., D* **2014**, *47* (14), 145201.
(172) Zhou, P.; Yang, Y.; Huang, G.; Lai, A. C. K. Numerical and experimental study on airborne disinfection by negative ions in air duct flow. *Build. Environ.* **2018**, *127*, 204−210.
(173) Feng, Z.; Cao, S. J.; Wang, J.; Kumar, P.; Haghighat, F. Indoor airborne disinfection with electrostatic disinfector (ESD): Numerical simulations of ESD performance and reduction of computing time. *Build. Environ.* **2021**, *200*, No. 107956.
(174) Kowalski, W.; Bahnfleth, W. P.; Witham, D.; Severin, B.; Whittam, T. Mathematical modeling of ultraviolet germicidal irradiation for air disinfection. *Quant. Biol.* **2000**, *2*, 249−270.
(175) Rudnick, S.; Milton, D. K. Risk of indoor airborne infection transmission estimated from carbon dioxide concentration. *Indoor Air* **2003**, *13* (3), 237−245.
(176) Nicas, M.; Nazaroff, W. W.; Hubbard, A. Toward understanding the risk of secondary airborne infection: emission of respirable pathogens. *J. Occup. Environ. Hyg.* **2005**, *2* (3), 143−154.
(177) Tang, J.; Li, Y.; Eames, I.; Chan, P.; Ridgway, G. Factors involved in the aerosol transmission of infection and control of ventilation in healthcare premises. *J. Hosp. Infect.* **2006**, *64* (2), 100−114.
(178) Xie, X.; Li, Y.; Chwang, A.; Ho, P.; Seto, W. How far droplets can move in indoor environments−revisiting the wells evaporation−falling curve. *Indoor Air* **2007**, *17* (3), 211−225.
(179) Buonanno, G.; Morawska, L.; Stabile, L. Quantitative assessment of the risk of airborne transmission of SARS-CoV-2 infection: prospective and retrospective applications. *Environ. Int.* **2020**, *145*, No. 106112.
(180) Chen, W.; Zhang, N.; Wei, J.; Yen, H.-L.; Li, Y. Short-range airborne route dominates exposure of respiratory infection during close contact. *Build. Environ.* **2020**, *176*, No. 106859.
(181) Bueno de Mesquita, P. J.; Delp, W. W.; Chan, W. R.; Bahnfleth, W. P.; Singer, B. C. Control of airborne infectious disease in buildings: Evidence and research priorities. *Indoor Air* **2022**, *32* (1), No. e12965.
(182) Wong, N. H.; Heryanto, S. The study of active stack effect to enhance natural ventilation using wind tunnel and computational fluid dynamics (CFD) simulations. *Energy Build.* **2004**, *36* (7), 668−678.
(183) Luongo, J. C.; Fennelly, K. P.; Keen, J. A.; Zhai, Z. J.; Jones, B. W.; Miller, S. L. Role of mechanical ventilation in the airborne transmission of infectious agents in buildings. *Indoor Air* **2016**, *26* (5), 666−678.
(184) Nielsen, P. V.; Xu, C. Multiple airflow patterns in human microenvironment and the influence on short-distance airborne cross-infection−A review. *Indoor Built Environ.* **2022**, *31* (5), 1161−1175.
(185) Feng, Z.; Cao, S. J.; Haghighat, F. Removal of SARS-CoV-2 using UV+Filter in built environment. *Sustain. Cities Soc.* **2021**, *74*, No. 103226.
(186) Izadyar, N.; Miller, W. Ventilation strategies and design impacts on indoor airborne transmission: A review. *Build. Environ.* **2022**, *218*, No. 109158.
(187) Ismail, I. M.; Rashid, M. I.; Ali, N.; Altaf, B. A. S.; Munir, M. Temperature, humidity and outdoor air quality indicators influence COVID-19 spread rate and mortality in major cities of Saudi Arabia. *Environ. Res.* **2022**, *204*, No. 112071.
(188) Han, S.; Li, Y.; Wen, G.; Huang, T. Study on thermophoretic deposition of micron-sized aerosol particles by direct numerical simulation and experiments. *Ecotox. Environ. Safe.* **2022**, *233*, No. 113316.
(189) Matida, E. A.; Finlay, W. H.; Breuer, M.; Lange, C. F. Improving prediction of aerosol deposition in an idealized mouth using large-eddy simulation. *J. Aerosol Med.* **2006**, *19* (3), 290−300.
(190) Lai, A. C.; Chen, F. Modeling particle deposition and distribution in a chamber with a two-equation Reynolds-averaged Navier−Stokes model. *J. Aerosol Sci.* **2006**, *37* (12), 1770−1780.
(191) Zhuang, C.; Yang, G.; Long, T.; Hu, D. Numerical comparison of removal and deposition for fully-distributed particles in central-and split-type air-conditioning rooms. *Build. Environ.* **2017**, *112*, 17−28.
(192) Ma, B.; Lutchen, K. R. CFD simulation of aerosol deposition in an anatomically based human large−medium airway model. *Ann. Biomed. Eng.* **2009**, *37*, 271−285.
(193) K S Narayanan, S. S.; Wang, X.; Paul, J.; Paley, V.; Weng, Z.; Ye, L.; Zhong, Y. Disinfection and Electrostatic Recovery of N95 Respirators by Corona Discharge for Safe Reuse. *Environ. Sci. Technol.* **2021**, *55* (22), 15351−15360.
(194) Lee, J.; Bong, C.; Lim, W.; Bae, P. K.; Abafogi, A. T.; Baek, S. H.; Shin, Y.-B.; Bak, M. S.; Park, S. Fast and Easy Disinfection of Coronavirus-Contaminated Face Masks Using Ozone Gas Produced by a Dielectric Barrier Discharge Plasma Generator. *Environ. Sci. Technol. Lett.* **2021**, *8* (4), 339−344.
(195) Park, M.; Son, A.; Chua, B. Microorganism-ionizing respirator with reduced breathing resistance suitable for removing airborne bacteria. *Sens. Actuators, B* **2018**, *276*, 437−446.
(196) Gao, Y.; Gu, Y.; Tian, E.; Mo, J. A two-stage cascaded ionizer for boosting PM charging in electrostatic filtration: Principles, design, and long-term performance. *Sep. Purif. Technol.* **2023**, *313*, No. 123494.
(197) Mo, J.; Gu, Y.; Tian, E. Efficiently remove submicron particles by a novel foldable electrostatically assisted air coarse filter. *Sep. Purif. Technol.* **2022**, *288*, No. 120631.
(198) Kchaou, M.; Abuhasel, K.; Khadr, M.; Hosni, F.; Alquraish, M. Surface Disinfection to Protect against Microorganisms: Overview of Traditional Methods and Issues of Emergent Nanotechnologies. *Appl. Sci.* **2020**, *10* (17), 6040.
(199) Peters, A.; Palomo, R.; Ney, H.; Lotfinejad, N.; Zingg, W.; Parneix, P.; Pittet, D. The COVID-19 pandemic and N95 masks: reusability and decontamination methods. *Antimicrob. Resist. Infect. Control* **2021**, *10* (1), 83.
(200) Niveditha, A.; Pandiselvam, R.; Prasath, V. A.; Singh, S. K.; Gul, K.; Kothakota, A. Application of cold plasma and ozone technology for decontamination of Escherichia coli in foods- a review. *Food Control* **2021**, *130*, No. 108338.
(201) Foster, J. E. Plasma-based water purification: Challenges and prospects for the future. *Phys. Plasmas* **2017**, *24* (5), No. 055501.
(202) Hosseini, S.; Moghaddas, H.; Masoudi Soltani, S.; Kheawhom, S. Technological Applications of Honeycomb Monoliths in Environmental Processes: A review. *Process Saf. Environ. Prot.* **2020**, *133*, 286−300.
(203) Tu, Y.; Tang, W.; Yu, L.; Liu, Z.; Liu, Y.; Xia, H.; Zhang, H.; Chen, S.; Wu, J.; Cui, X.; et al. Inactivating SARS-CoV-2 by electrochemical oxidation. *Sci. Bull.* **2021**, *66* (7), 720−726.
(204) Miklos, D. B.; Remy, C.; Jekel, M.; Linden, K. G.; Drewes, J. E.; Hübner, U. Evaluation of advanced oxidation processes for water and wastewater treatment−A critical review. *Water Res.* **2018**, *139*, 118−131.
(205) Lynn, W.; Heffron, J.; Mayer, B. K. Electrocoagulation as a Pretreatment for Electroxidation of *E. coli*. *Water* **2019**, *11* (12), 2509.
(206) Gallagher, M. J.; Vaze, N.; Gangoli, S.; Vasilets, V. N.; Gutsol, A. F.; Milovanova, T. N.; Anandan, S.; Murasko, D. M.; Fridman, A. A. Rapid inactivation of airborne bacteria using atmospheric pressure dielectric barrier grating discharge. *IEEE Trans. Plasma Sci.* **2007**, *35* (5), 1501−1510.

(207) Wang, J.; Zhang, Y.; Kuang, L.; Yang, J.; Xu, C.; Mu, B.; Li, J.; Lu, P.; Song, W.; Wang, W.; Wu, A.; Liang, X.; Zhang, J. Low-voltage driven Ag-Co3O4 textile device for multifunctional air cleaning. *Chem. Eng. J.* **2021**, *424*, No. 130320.

(208) Gupta, A.; Sharma, C. P.; Thamaraiselvan, C.; Pisharody, L.; Powell, C. D.; Arnusch, C. J. Low-voltage bacterial and viral killing using laser-induced graphene-coated non-woven air filters. *ACS Appl. Mater. Interfaces* **2021**, *13* (49), 59373−59380.

(209) Jin, L.; Chen, M.; Chen, Z.; Li, M.; Yao, M.; Lu, Y. Efficient Air Disinfection Achieved by Nanowire-Modified Copper Mesh Electrodes. *ACS ES&T Engg.* **2024**, *4* (6), 1422−1432.

(210) Park, M.; Son, A.; Chua, B. Microorganism-ionizing respirator with reduced breathing resistance suitable for removing airborne bacteria. *Sens. Actuators, B* **2018**, *276*, 437−446.

(211) Gu, G. Q.; Han, C. B.; Tian, J. J.; Jiang, T.; He, C.; Lu, C. X.; Bai, Y.; Nie, J. H.; Li, Z.; Wang, Z. L. Triboelectric nanogenerator enhanced multilayered antibacterial nanofiber air filters for efficient removal of ultrafine particulate matter. *Nano Res.* **2018**, *11*, 4090−4101.

(212) Prehn, F.; Timmermann, E.; Kettlitz, M.; Schaufler, K.; Günther, S.; Hahn, V. Inactivation of airborne bacteria by plasma treatment and ionic wind for indoor air cleaning. *Plasma Process. Polym.* **2020**, *17* (9), No. 2000027.

(213) Xia, T.; Yang, M.; Marabella, I.; Lee, E.; Olson, B.; Zarling, D.; Torremorell, M.; Clack, H. Inactivation of airborne porcine reproductive and respiratory syndrome virus (PRRSv) by a packed bed dielectric barrier discharge non-thermal plasma. *J. Hazard. Mater.* **2020**, *393*, No. 122266.

(214) Martínez-Montelongo, J. H.; Medina-Ramírez, I. E.; Romo-Lozano, Y.; Zapien, J. A. Development of a sustainable photocatalytic process for air purification. *Chemosphere* **2020**, *257*, No. 127236.

(215) Mainka, A.; Mucha, W.; Pastuszka, J. S.; Bragoszewska, E.; Janoszek, A. Non-commercial Air Purifier—The Effectiveness and Safety. *Buildings* **2020**, *10* (6), 104.

(216) Mudway, I. S.; K, F. J. Ozone and the lung: a sensitive issue. *Molecular Aspects of Medicine* **2000**, *21* (1−2), 1−48. Organization, W. H.; Environment, W. E. C. f. *WHO global air quality guidelines: particulate matter (PM2. 5 and PM10), ozone, nitrogen dioxide, sulfur dioxide and carbon monoxide*; World Health Organization, 2021.

(217) Yao, X.; Li, Y.; Fan, Z.; Zhang, Z.; Chen, M.; Shangguan, W. Plasma Catalytic Removal of Hexanal over Co−Mn Solid Solution: Effect of Preparation Method and Synergistic Reaction of Ozone. *Ind. Eng. Chem. Res.* **2018**, *57* (12), 4214−4224.

(218) Zhang, Y.; Chen, M.; Zhang, Z.; Jiang, Z.; Shangguan, W.; Einaga, H. Simultaneously catalytic decomposition of formaldehyde and ozone over manganese cerium oxides at room temperature: Promotional effect of relative humidity on the MnCeOx solid solution. *Catal. Today* **2019**, *327*, 323−333.

(219) Zhang, Y.; Shi, J.; Fang, W.; Chen, M.; Zhang, Z.; Jiang, Z.; Shangguan, W.; Einaga, H. Simultaneous catalytic elimination of formaldehyde and ozone over one-dimensional rod-like manganese dioxide at ambient temperature. *J. Chem. Technol. Biotechnol.* **2019**, *94* (7), 2305−2317.

(220) Afshari, A.; Ekberg, L.; Forejt, L.; Mo, J.; Rahimi, S.; Siegel, J.; Chen, W.; Wargocki, P.; Zurami, S.; Zhang, J. Electrostatic Precipitators as an Indoor Air Cleaner—A Literature Review. *Sustainability* **2020**, *12* (21), 8774.

(221) Viner, A.S.; Lawless, P.A.; Ensor, D.S.; Sparks, L.E. Ozone generation in DC-energized electrostatic precipitators. *IEEE Trans. Ind. Appl.* **1992**, *28* (3), 504−512.

(222) Boelter, K. J.; Davidson, J. H. Ozone Generation by Indoor, Electrostatic Air Cleaners. *Aerosol Sci. Technol.* **1997**, *27* (6), 689−708.

(223) Bo, Z.; Yu, K.; Lu, G.; Mao, S.; Chen, J.; Fan, F.-g. Nanoscale Discharge Electrode for Minimizing Ozone Emission from Indoor Corona Devices. *Environ. Sci. Technol.* **2010**, *44* (16), 6337−6342.

(224) Yun, S. J.; Min, B. R.; Seo, Y. A novel polymer-arrayed electrostatic precipitator with electrical resistance material for the removal of fine particles. *J. Aerosol Sci.* **2013**, *57*, 88−95.

(225) Sung, J.-H.; Lee, Y.; Han, B.; Kim, Y.-J.; Kim, H.-J. Improvement of particle clean air delivery rate of an ion spray electrostatic air cleaner with zero-ozone based on diffusion charging. *Build. Environ.* **2020**, *186*, No. 107335.

(226) Ye, J.; Li, J.; Chen, X.; Huang, S.; Ou-Yang, W. Enhancement of corona discharge induced wind generation with carbon nanotube and titanium dioxide decoration. *Chin. Phys. B* **2019**, *28* (9), No. 095202.

(227) Dorsey, J.A.; Davidson, J.H. Ozone production in electrostatic air cleaners with contaminated electrodes. *IEEE Trans. Ind. Appl.* **1994**, *30* (2), 370−376.

(228) Morrison, G. C.; Shaughnessy, R.; Siegel, J. *In-duct air cleaning devices: ozone emission rates and test methodology*; California Air Resources Board, Research Division Sacramento, CA, USA, 2014.

(229) Liu, L.; Guo, J.; Li, J.; Sheng, L. The effect of wire heating and configuration on ozone emission in a negative ion generator. *J. Electrost.* **2000**, *48* (2), 81−91.

(230) Tanasomwang, L.; Lai, F. Long-term ozone generation from electrostatic air cleaners. *IEEE Trans. Ind. Appl.* **1997**, *3*, 2037−2044.

(231) Tian, E.; Xia, F.; Wu, J.; Zhang, Y.; Li, J.; Wang, H.; Mo, J. Electrostatic Air Filtration by Multifunctional Dielectric Heterocaking Filters with Ultralow Pressure Drop. *ACS Appl. Mater. Interfaces* **2020**, *12* (26), 29383−29392.

(232) Waring, M. S.; Siegel, J. A. The effect of an ion generator on indoor air quality in a residential room. *Indoor Air* **2011**, *21* (4), 267−276.

(233) Zhang, Y.; Mo, J.; Li, Y.; Sundell, J.; Wargocki, P.; Zhang, J.; Little, J. C.; Corsi, R.; Deng, Q.; Leung, M. H.K.; Fang, L.; Chen, W.; Li, J.; Sun, Y. Can commonly-used fan-driven air cleaning technologies improve indoor air quality? A literature review. *Atmos. Environ.* **2011**, *45* (26), 4329−4343.

(234) Joo, T.; Rivera-Rios, J. C.; Alvarado-Velez, D.; Westgate, S.; Ng, N. L. Formation of Oxidized Gases and Secondary Organic Aerosol from a Commercial Oxidant-Generating Electronic Air Cleaner. *Environ. Sci. Technol. Lett.* **2021**, *8* (8), 691−698.

(235) Zeng, Y.; Manwatkar, P.; Laguerre, A.; Beke, M.; Kang, I.; Ali, A. S.; Farmer, D. K.; Gall, E. T.; Heidarinejad, M.; Stephens, B. Evaluating a commercially available in-duct bipolar ionization device for pollutant removal and potential byproduct formation. *Build. Environ.* **2021**, *195*, No. 107750.

(236) Licht, S.; Hehir, A.; Trent, S.; Dunlap, D.; Borumand, K.; Wilson, M.; Smith, K. *Use of Bipolar Ionization for Disinfection within Airplanes*. Boeing: Chicago, IL, USA, 2021.

https://doi.org/10.1021/envhealth.4c00100
Environ. Health 2024, 2, 596−617